

ADVANCED REVIEW

Journal Section

arXiv:2504.09724v2 [cs.CV] 23 May 2025

A Survey on Efficient Vision-Language Models

Gaurav Shinde[‡] | Anuradha Ravi[^] | Emon Dey[^] |
Shadman Sakib[^] | Milind Rampure[^] | Nirmalya Roy[^]

[^]Mobile Pervasive & Sensor Computing Lab and Department of Information Systems, University of Maryland Baltimore County (UMBC), Baltimore, Maryland, 21250, USA

Correspondence

[‡]Gaurav Shinde,
Mobile Pervasive & Sensor Computing Lab and Department of Information Systems, University of Maryland Baltimore County (UMBC), Baltimore, Maryland, 21250, USA
Email: gshinde1@umbc.edu

Present address

Mobile Pervasive & Sensor Computing Lab and Department of Information Systems, University of Maryland Baltimore County (UMBC), Baltimore, Maryland, 21250, USA

Funding information

This work has been partially supported by NSF CAREER Award # 1750936, NSF REU Site Grant # 2050999, NSF CNS EAGER Grant # 2233879, and ONR Grant # N00014-23-1-2119

Vision-language models (VLMs) integrate visual and textual information, enabling a wide range of applications such as image captioning and visual question answering, making them crucial for modern AI systems. However, their high computational demands pose challenges for real-time applications. This has led to a growing focus on developing efficient vision-language models. In this survey, we review key techniques for optimizing VLMs on edge and resource-constrained devices. We also explore compact VLM architectures, frameworks and provide detailed insights into the performance-memory trade-offs of efficient VLMs. Furthermore, we establish a GitHub repository at [MPSC-GitHub](#) to compile all surveyed papers, which we will actively update. Our objective is to foster deeper research in this area.

KEYWORDS

Efficient Vision Language Models, Multimodal Models, Edge Devices

1 | INTRODUCTION

Vision-Language Models (VLMs) have emerged as a response to the growing need for systems that can process and integrate visual and textual data effectively. The increasing availability of multimodal data across domains such as healthcare (medical images paired with diagnostic reports), autonomous systems (sensor feeds integrated with navigation commands), and social media (images combined with captions) highlighted the limitations of unimodal models, which struggled to connect visual content with its linguistic context. VLMs address this challenge by aligning vision and text in a shared representation space which enables advanced capabilities in tasks such as image captioning, cross-modal retrieval, visual question answering (VQA) and visual commonsense reasoning (VCR). Advances in deep learning architectures and the availability of large-scale multimodal datasets have further fueled the development of VLMs.

VLMs leverage diverse objectives to align and integrate multimodal data effectively, with approaches such as contrastive learning, masked modeling, and generative modeling playing a pivotal role. In contrastive-based VLMs, the goal

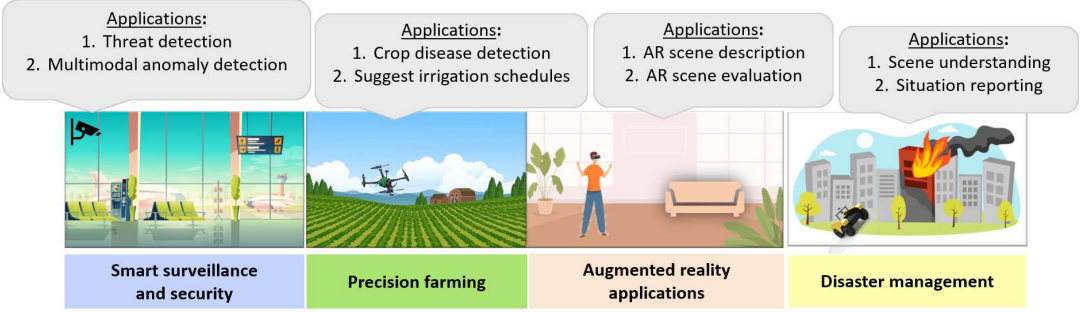


FIGURE 1 Key VLM applications highlighting the necessity of edge deployment.

is to assign low energy to consistent data pairs while penalizing unlikely combinations with higher energy. The learned energy function $E_\phi(x)$ maps these data samples into a probability distribution using the Boltzmann formula:

$$P_\phi(x) = \frac{e^{-E_\phi(x)}}{\sum_x e^{-E_\phi(x)}}. \quad (1)$$

This ensures that samples with lower energy correspond to higher probabilities. The objective is to align $P_\phi(x)$ the model's distribution with $P_T(x)$ the target distribution. This optimization often involves the maximum likelihood estimation, with gradients computed over positive and negative samples, where negative samples are synthesized through methods like Markov Chain Monte Carlo (MCMC). Models like CLIP [Radford et al. \(2021\)](#) and SigLIP [Zhai et al. \(2023\)](#) demonstrate the effectiveness of contrastive learning by aligning visual and textual embeddings in a shared representation space, enabling robust performance across a wide range of multimodal tasks. Masked modeling offers a different approach by masking parts of the input and training the model to predict the masked portion. Masked Language Modeling (MLM), for example, benefits from the transformer architecture by strategically dropping input tokens and predicting them, while Masked Image Modeling (MIM) employs similar principles for visual data. Frameworks like FLAVA [Singh et al. \(2022\)](#) and BEiT [Bao et al. \(2021\)](#) effectively utilize masked modeling to pre-train on vast multimodal datasets. Generative models, on the other hand, extend the capabilities of VLMs by simultaneously learning contrastive and generative losses. Generative models are widely used for image captioning tasks. CM3Leon [Yu et al. \(2023b\)](#) utilizes distinct image and text tokenizers to convert respective modalities into token sequences, which are subsequently processed by a transformer decoder. In contrast, Chameleon [Team \(2024\)](#) extends this framework by employing the same transformer model for processing both image and text tokens to ensure a unified and efficient design. Although widely applied to image captioning tasks, generative models can also be utilized for various downstream applications. For example, they can be employed for image classification tasks using Bayes' rule. The probability for a given label y given an image x can be expressed as:

$$P(y|x) = \frac{P(x|y)P(y)}{P(x)}. \quad (2)$$

To optimize computational resources and reduce training costs, VLMs often integrate pre-trained backbones such as Frozen [Tsimpoukelli et al. \(2021\)](#), MiniGPT [Zhu et al. \(2023\)](#), or the Qwen series [Qwen et al. \(2024\)](#). These pretrained components accelerate convergence and generalize effectively across tasks. VLM pre-training frameworks differ in architecture, ranging from two-tower VLMs with distinct encoders for image and text to one-tower VLMs that utilize unified networks to generate joint embeddings. These approaches enhance the efficiency of VLMs, making them useful for edge device applications.

The deployment of VLMs on resource-constrained devices addresses the growing need for real-time processing and privacy preservation by enabling on-device computations. Furthermore, edge deployment ensures seamless performance in environments with limited or unreliable network connectivity, making VLMs highly adaptable for applications like autonomous navigation and smart IoT systems (figure 1). As state-of-the-art VLMs grow in complexity to achieve higher performance, their memory footprint and inference latency have increased significantly. For example, the CLIP-

B/16 model Liu (2024) consists of 86.2M parameters for the image encoder and 63.4M parameters for the text encoder, making them unsuitable for deployment on edge devices such as the Jetson Nano (4 GB RAM, no dedicated GPU) or even the Jetson Xavier (8 GB RAM, 1 GPU). On a Jetson Nano, the limited RAM would cause frequent memory swaps, severely impacting latency and throughput, while on the Jetson Xavier, the GPU may still struggle to handle the large model's computational demands in real-time applications. These limitations emphasize the critical need for efficient VLMs that optimize memory usage and latency while maintaining competitive performance.

The main contributions of this survey are threefold. ❶ We present various techniques, including pre-deployment, efficient fine-tuning, and runtime optimizations, to enhance the efficiency of VLMs for resource-constrained devices. ❷ We list state-of-the-art lightweight VLMs and discuss various frameworks. ❸ We provide detailed insights into the performance-memory trade-off for certain VLMs using the techniques discussed.

This survey is structured around the taxonomy illustrated in Figure 2. While existing surveys such as Ghosh et al. (2024) primarily explore various VLM architectures and Du et al. (2022) delve into Vision-Language Pre-Trained Models (VL-PTMs) and Zhang et al. (2024a) mention techniques like knowledge distillation and transfer learning, our work provides an in-depth analysis of efficient VLMs specifically tailored for edge and resource-constrained devices. Table 1 compares our survey with similar ones. To ensure a thorough review we sourced relevant papers from leading conferences and workshops using platforms such as Google Scholar, DBLP and ResearchGate. Keywords such as "VLM quantization," "VLM pruning," "VLM finetuning techniques," "VLM knowledge distillation," and "VLM runtime optimizations" guided our literature search, enabling a targeted exploration of this rapidly evolving field.

The rest of the survey is organized as follows. Section 2 covers pre-deployment techniques for efficient VLMs, while Sections 3 and 4 detail fine-tuning and runtime optimization methods. Section 5 explores distributed VLMs. Section 6 lists state-of-the-art, efficient VLMs and also details various VLM frameworks and libraries. Section 7 provides insights into the accuracy vs. efficiency trade-offs for VLMs. Section 8 outlines application avenues, Section 9 discusses challenges and future directions, and Section 10 concludes the paper.

We also create a **GitHub repository** to compile the papers featured in this survey: [MPSC-GitHub](#). It will be actively maintained with updates on emerging research.

TABLE 1 Comparison of our survey with similar ones; ● means full coverage of the topic, ◐ means partial coverage of the topic, and ○ means no coverage.

Reference	Pre-deployment Techniques	Efficient Fine-tuning Techniques	Runtime Optimization	Security and Privacy	Applications	Memory vs. Performance Insights
Xing et al. (2024a)	○	●	○	●	○	○
Jin et al. (2024)	◐	●	○	○	●	○
Sharshar et al. (2025)	◐	●	◐	●	●	○
Zhang et al. (2024b)	◐	◐	○	○	◐	○
<u>Ours</u>	●	●	●	●	●	●

2 | PRE-DEPLOYMENT TECHNIQUES

Pre-deployment techniques refer to optimization methods applied to models before deployment to improve their efficiency while maintaining accuracy. In our survey, we focus on techniques such as quantization, low-rank approximation, pruning, and knowledge distillation. These methods are particularly suited for edge devices as they reduce computational and memory requirements. The most commonly used benchmarked datasets for evaluating these methods include ScienceQA Lu et al. (2022), VQA-v2 Goyal et al. (2019a), MMMU Yue et al. (2024a), SEED Li et al. (2023), and OCRBench Liu et al. (2024b). The primary evaluation metrics are accuracy, top-1 accuracy, and the harmonic mean, as employed in Q-VLM Wang et al. (2024), MBQ Li et al. (2024b), MoPE-CLIP Lin et al. (2024a), and PromptKD Li et al. (2024e). Inference latency and memory consumption are commonly used to assess the efficiency of these approaches.

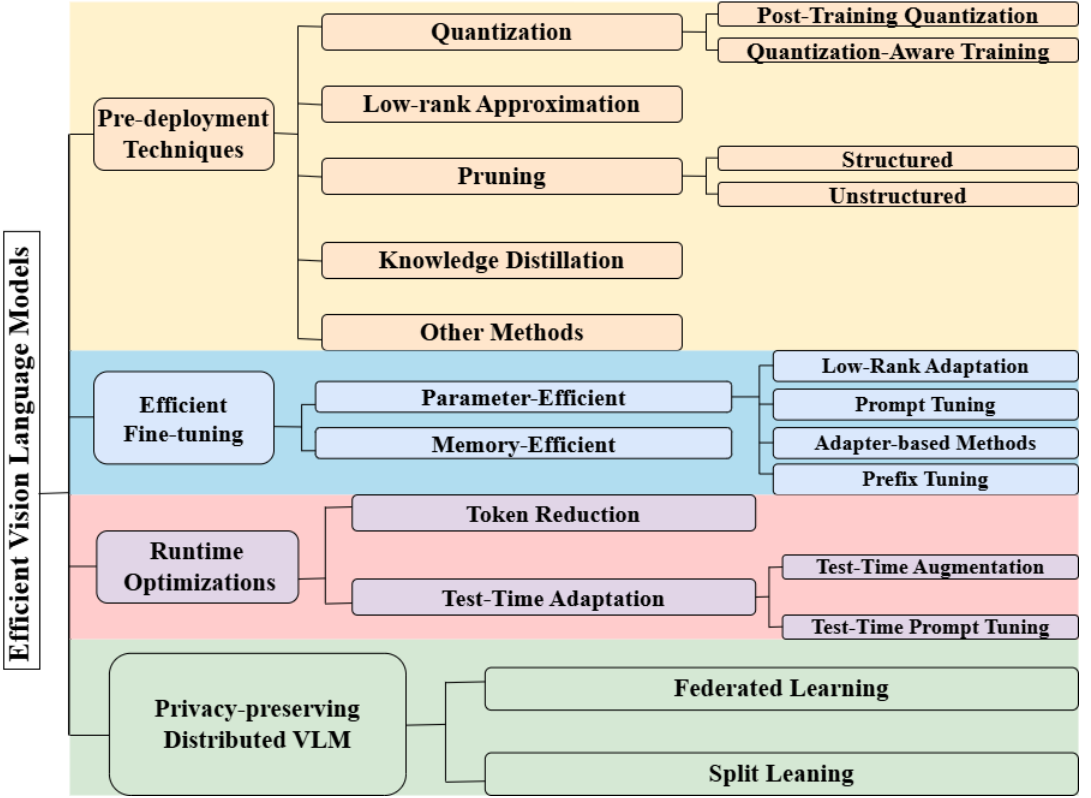


FIGURE 2 Taxonomy of efficient vision-language models (VLMs).

Training is typically conducted on high-performance GPUs such as the RTX 4090, V100, and A100.

2.1 | Quantization

Quantization refers to the compression of weights and activations by reducing their precision, which enables computational efficiency. Quantization minimizes memory footprint while maintaining accuracy as it maps continuous values x (e.g., in FP32) to discrete values $q(x)$ in lower-bit formats. In terms of precision, FP32 provides 7 digits of accuracy, FP16 reduces this to 3-4 decimal places, while INT8 eliminates decimals entirely. Despite the lower precision, INT8 quantization is effective because it optimizes the numerical range required for model parameters rather than mapping the entire range of floating-point values. For example, mapping FP32 values $[-3.4 \times 10^{38}, 3.4 \times 10^{38}]$ to the INT8 range $[-128, 127]$ allows efficient representation of the model's parameter range while significantly reducing computational complexity. Quantization improves hardware efficiency as NVIDIA GPUs use tensor cores optimized for faster and cheaper lower-bit operations like INT8 compared to FP32. This delivers high throughput, making it beneficial for resource-limited layers. Quantization methods can be categorized into symmetric and asymmetric approaches. Symmetric quantization maps the range of floating-point values symmetrically around zero. The scale factor η is computed as:

$$\eta = \frac{2^{n-1} - 1}{\beta}. \quad (3)$$

where β is the maximum absolute value, and n represents the number of bytes to be quantized. The quantized value $q(v)$ is then calculated as:

$$q(v) = \text{round}(\eta \cdot v). \quad (4)$$

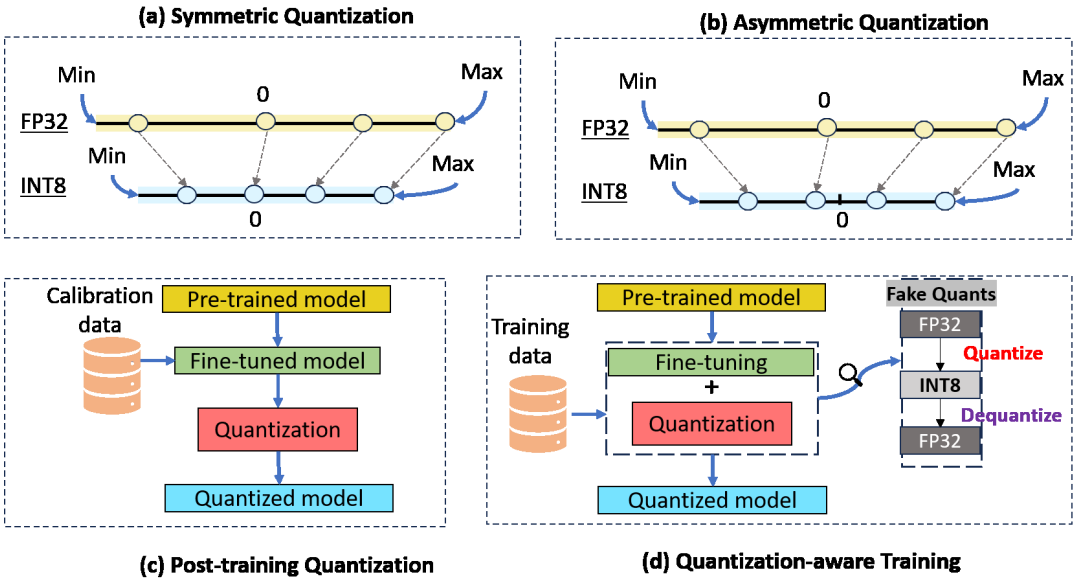


FIGURE 3 Overview of quantization: symmetric and asymmetric methods alongside post-training quantization (PTQ) and quantization-aware training (QAT) approaches.

This approach ensures that zero remains zero in the quantized space, while maintaining symmetry around the origin. Asymmetric quantization introduces a shift γ (zero-point) to handle distributions not centered around zero. The quantized value $q(v)$ is defined as:

$$q(v) = \text{round}(\eta \cdot v + \gamma). \quad (5)$$

Here, the scale factor η and offset γ are calculated as:

$$\eta = \frac{\theta_{\max} - \theta_{\min}}{2^n - 1}, \quad \gamma = \text{round}(-\eta \cdot \theta_{\min}). \quad (6)$$

where θ_{\max} and θ_{\min} are the maximum and minimum values of the floating point range. Quantization is broadly classified into Post-Training Quantization (PTQ) and Quantization-Aware Training (QAT). Figure 3 illustrates these approaches.

2.1.1 | Post-Training Quantization (PTQ)

PTQ updates the weights and activations after training using a small dataset, employing either symmetric or asymmetric methods. It is simpler for weights due to direct access to weight tensors but more challenging for activations as they require measurement with input data. This requires innovative techniques to balance efficiency and accuracy, especially when handling the complexities of activation quantization. Wang et al. (2024) propose Q-VLM, a PTQ framework for large vision-language models (LVLMs) that focuses on minimizing cross-layer dependency errors using activation entropy as a proxy. This method partitions the model into blocks for efficient quantization and employs visual encoder optimization to reduce search space while maintaining accuracy. It achieves significant memory compression and faster inference speeds without performance degradation. Li et al. (2024b) introduces Modality-Balanced Quantization (MBQ) for LVLMs that accounts for sensitivity differences between vision and language tokens. By balancing reconstruction loss during calibration, MBQ improves accuracy and supports weight-only and weight-activation coquantization, achieving up to 1.4× decoding speedup with a custom W3 kernel. NoisyQuant Liu et al. (2023b) reshapes activation distributions using uniform noisy bias to reduce quantization errors in vision transformers and can be adapted to VLMs for efficient activation quantization. To mitigate the performance drop problem in PTQ, P4Q Sun et al. (2024) introduces

learnable prompts and a lightweight low-bit adapter to realign image and text feature distributions. This approach enhances recognition performance and achieves results comparable to full-precision models while maintaining computational efficiency. Some PTQ methods are specifically designed for vision and language models independently; however, they can also be applied to vision and language components within VLMs. Therefore, it is essential to consider these methods when discussing PTQ strategies for VLMs. [Liu et al. \(2021\)](#) propose a PTQ method tailored for vision transformers, introducing similarity- and ranking-aware objectives to preserve attention behavior without fine-tuning. They also use mixed-precision quantization based on nuclear norms, achieving near-full precision accuracy (81.29% top-1 on ImageNet with DeiT-B) while significantly reducing model size and latency. [Lin et al. \(2022\)](#) present FQ-ViT as a post-training method that enables fully quantized vision transformers by addressing LayerNorm and Softmax issues using Power-of-Two Factor (PTF) and Log-Int-Softmax (LIS). This approach achieves 84.89% top-1 accuracy with ViT-L on ImageNet. [Zhang et al. \(2025b\)](#) introduce SageAttention, a plug-and-play PTQ method that quantizes the attention module in Transformers. It achieves INT8 quantization of attention while preserving accuracy through innovations like smoothing the K matrix and using FP16 accumulators, resulting in up to $2.1\times$ faster inference compared to FlashAttention2 [Dao \(2024\)](#) across various models. Building on this, SageAttention2 [Zhang et al. \(2025a\)](#) further accelerates attention using INT4 per-thread quantization alongside precision-enhancing techniques such as Q-smoothing and two-level accumulation. It achieves up to $3\times$ faster inference than FlashAttention2 while maintaining end-to-end accuracy across language, image, and video generation models. [Yuan et al. \(2022\)](#) propose twin uniform quantization for vision transformers to handle the special distributions of activations and a Hessian-guided metric to improve scaling factor selection. This can enhance the efficiency of transformer-based vision encoders in VLMs while maintaining near-lossless accuracy. Similarly, [Lv et al. \(2024\)](#) develop PTQ4SAM, a quantization framework for the Segment Anything Model (SAM), which incorporates a Bimodal Integration strategy to address challenging activation distributions and Adaptive Granularity Quantization to improve softmax quantization. PTQ techniques such as LRQuant and BiLLM offer promising solutions for compressing language components in VLMs. LRQuant [Zhao et al. \(2024\)](#) enhances learnability and generalization through dynamic smoothing and test-time adaptation, while BiLLM [Huang et al. \(2025\)](#) improves and extends ultra-low-bit quantization to minimize memory and computation costs. SmoothQuant [Xiao et al. \(2023\)](#) enables training-free quantization for LLMs by smoothing activation outliers and balancing quantization difficulty via per-channel scaling, achieving W8A8 quantization with up to $1.56\times$ speedup and minimal accuracy loss across models up to 530B on a single node.

2.1.2 | Quantization-Aware Training (QAT)

QAT occurs during training itself, allowing the model to fine-tune with quantized weights and achieve better performance than PTQ. Fake quantization is applied in the forward pass, making the model adapt to quantization effects while retaining the full precision version. Very few studies have directly investigated this approach in the context of VLMs. [Xie et al. \(2024a\)](#) introduce QSLAW, a quantization-aware scale learning approach for VLMs, optimizing multimodal large language models (MLLMs) by learning group-wise scale factors to mitigate quantization errors. Additionally, it uses a modality-aware warmup approach to enhance VL instruction tuning efficiency while preserving linguistic knowledge. Most studies have focused on either the vision or language component, but surveying these methods is valuable as they can be applied separately. [Huang et al. \(2024b\)](#) identify quantization variation as a key challenge in transformer QAT and propose a variation-aware scheme combining module-dependent scaling, oscillation-aware regularization, and knowledge distillation to achieve state-of-the-art low-bit performance with improved training efficiency. Fixed-point ViT [Li et al. \(2021\)](#) introduces an enhanced QAT strategy by combining mean-square error-based initialization with learned step size quantization, achieving nearly-lossless 8-bit quantization. Q-ViT [Li et al. \(2022b\)](#) proposes a fully differentiable QAT framework for Vision Transformers, optimizing both quantization scales and bit-widths dynamically. It employs head-wise bit-width allocation and a switchable scale mechanism to enhance quantization robustness, achieving 3-bit precision with minimal accuracy loss. GPUSQ-ViT [Yu et al. \(2023a\)](#) employs sparse distillation-aware QAT to optimize

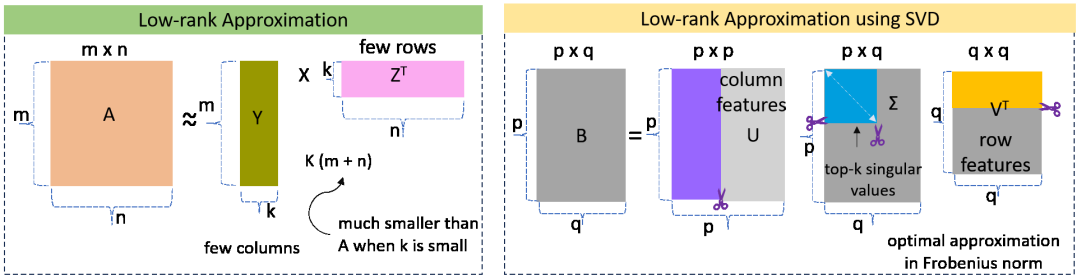


FIGURE 4 Schematic representation of low-rank approximation and SVD.

Vision Transformers for GPU efficiency. By integrating feature-based knowledge distillation with quantization scaling, it minimizes accuracy degradation while achieving substantial reductions in model size. PackQVIT [Dong et al. \(2023\)](#) introduces activation-aware sub-8-bit QAT with log2 and outlier-aware quantization, achieving real-time ViT inference and superior accuracy on mobile devices. LLM-QAT [Liu et al. \(2023c\)](#) leverages self-generated data from the pre-trained model for knowledge distillation, enabling QAT without access to the original dataset. It quantizes weights, activations, and the KV cache and significantly improves performance over PTQ methods. [Chen et al. \(2024b\)](#) employs QAT (EfficientQAT) to optimize LLMs by introducing block-wise training of all parameters (Block-AP) and end-to-end training of quantization parameters (E2E-QP). This approach reduces memory overhead and training time while maintaining high accuracy in low-bit quantization scenarios. QA-LoRA [Xu et al. \(2023\)](#) applies group-wise quantization alongside low-rank adaptation. This balances the flexibility between quantization and adaptation, enabling efficient training and deployment without the need for post-training quantization. LR-QAT [Bondarenko et al. \(2024\)](#) is a lightweight, memory-efficient QAT method for LLMs that combines low-rank adaptation with fixed-point downcasting and checkpointing. It achieves full-model QAT performance with minimal overhead and also supports various quantization settings.

2.2 | Low-rank Approximation

Low-rank approximation is a mathematical technique that reduces the number of parameters in a model. It discovers latent patterns and eliminates redundancy. The model becomes more efficient as a result of this reduction. The key idea is to shrink large matrices while retaining most of their information (for example, a 5000×5000 weight matrix can be approximated using 5000×500 and 500×5000 matrices, reducing the number of parameters from 25 million to 500 thousand). Matrix "A" can be approximated as follows:

$$A \approx YZ^T. \quad (7)$$

where each column of A is a linear combination of the columns of Y and each row of A is a linear combination of the rows of Z^T .

Low-rank approximation is widely used for image compression [Kumar et al. \(2022\)](#), denoising [Guo et al. \(2019\)](#) and matrix completion [Nie et al. \(2019\)](#). It offers several advantages, such as reduced memory consumption and computational efficiency, making it well suited for deployment on smartphones and IoT devices. It also reduces inference latency, thus enhancing real-time performance. However, the choice of rank is crucial when deploying on resource-constrained devices, as it directly impacts the compression ratio and the overall model performance. The rank- k approximation of a matrix B is computed by decomposing it into its singular value components and retaining only the k most significant ones (singular value decomposition (SVD) [Klema and Laub \(1980\)](#) is one such optimal method [4](#)):

$$B_k = \sum_{i=1}^k s_i u_i v_i^T. \quad (8)$$

where s_i are the singular values of B , sorted in descending order, and u_i and v_i are the corresponding left and right singular vectors.

Low-rank approximation has been widely used for language models and has recently been applied to multimodal models as well. Song et al. (2024a) introduce LoRA-Sparse, a low-rank approximation method for sparse attention in LLMs and multimodal models like LLaVA. LoRA-Sparse employs order-mimic training to approximate full attention effectively, demonstrating benefits across NLP and multimodal benchmarks. SeTAR Li et al. (2024c) proposes a training-free selective low-rank approximation method for Out of Distribution (OOD) detection in CLIP-based models, enhancing efficiency and accuracy without requiring fine-tuning. SeTAR+FT Li et al. (2024c) extends this by integrating fine-tuning for further performance gains, achieving state-of-the-art results on ImageNet1K and Pascal-VOC benchmarks. PELA Guo et al. (2024) incorporates an intermediate pre-training stage with low-rank approximation to compress pre-trained models. It enables efficient fine-tuning by distilling features and regularizing weight perturbations to improve scalability for downstream tasks.

2.3 | Pruning

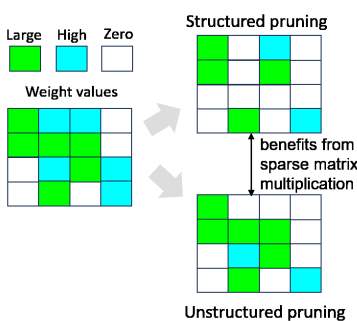


FIGURE 5 Illustration of structured and unstructured pruning.

Pruning is categorized into Structured and Unstructured Pruning. A schematic representation for the same is shown in figure 5.

Parameter pruning involves removing redundant or less significant model weights. A simple yet effective pruning method is to remove model weights that fall below a predetermined threshold. This thresholding approach is often referred to as magnitude pruning and serves as the basis for many iterative pruning strategies. However, more advanced techniques exist, such as gradient-based pruning, which evaluates weight importance based on sensitivity to loss function, and Hessian-based pruning that uses second-order information to identify less impactful weights. Parameter pruning reduces the memory footprint and computational load of large networks, making them more efficient for resource-constrained devices. By eliminating redundant weights, pruning enables faster inference, lower power consumption, and efficient deployment on edge devices. Pruning is categorized into Structured and Unstructured Pruning. A schematic representation for the

2.3.1 | Structured Pruning

This pruning technique uses a structured strategy to target sub-blocks, rows, or columns. This reduces computational complexity during the forward pass of the weight graph. As a result, hardware utilization becomes more efficient. For example, Lin et al. (2024a) introduce MoPE-CLIP, a mask-free structured pruning framework for VLMs, using the Module-Wise Pruning Error (MoPE) metric to assess module importance for cross-modal tasks. It optimizes model compression while preserving performance through width to depth pruning and knowledge distillation. In order to improve the scalability of structured pruning in VLMs and remove the need for costly fine-tuning, Meng et al. (2024) develop OSSCAR, a combinatorial optimization framework that uses low-rank updates and layer-wise reconstruction for efficient local search. Existing Transformer-based VLMs suffer from computational inefficiencies due to redundant token representations and attention heads, leading to high inference costs. To address this Wang et al. (2023d) propose SmartTrim an adaptive pruning framework that dynamically trims tokens and attention heads based on cross-modal complexity, ensuring efficient computation while maintaining performance across diverse tasks. Similarly, Transformer models consist of heterogeneous sub-structures making global pruning unreliable. To tackle this, Fang et al. (2024) introduce Isomorphic Pruning, which groups isomorphic sub-structures based on computational topology. This leads to reliable pruning.

2.3.2 | Unstructured Pruning

In this method, individual model weights are pruned. Unstructured pruning offers more flexibility compared to its structured counterpart and experiences a lower accuracy drop. However, this causes non-zero weights to be distributed unevenly, which results in irregular sparsity. Edge hardware is optimized for dense matrix operations, but unpredictable non-zero weight values can lead to frequent cache misses. To address this, various sparsification methods are being investigated and hardware accelerators are being improved. Some studies have explored unstructured pruning for VLMs. For example, [Yi-Lin Sung \(2024\)](#) introduces a two-stage coarse-to-fine layer-wise unstructured pruning approach that first determines sparsity ratios using a global importance score and then performs local pruning. This approach uses zeroth-order gradient approximations to reduce computational overhead while maintaining model performance across a variety of multimodal datasets. To solve the challenge of task-agnostic pruning and preserving multimodal transferability, MULTIFLOW [Farina et al. \(2024d\)](#) presents a gradient-free pruning framework that ranks parameter importance based on both magnitude and information flow. Also, [He et al. \(2024\)](#) reveal that unstructured pruning in VLMs significantly degrades performance beyond 50% sparsity.

2.4 | Knowledge Distillation (KD)

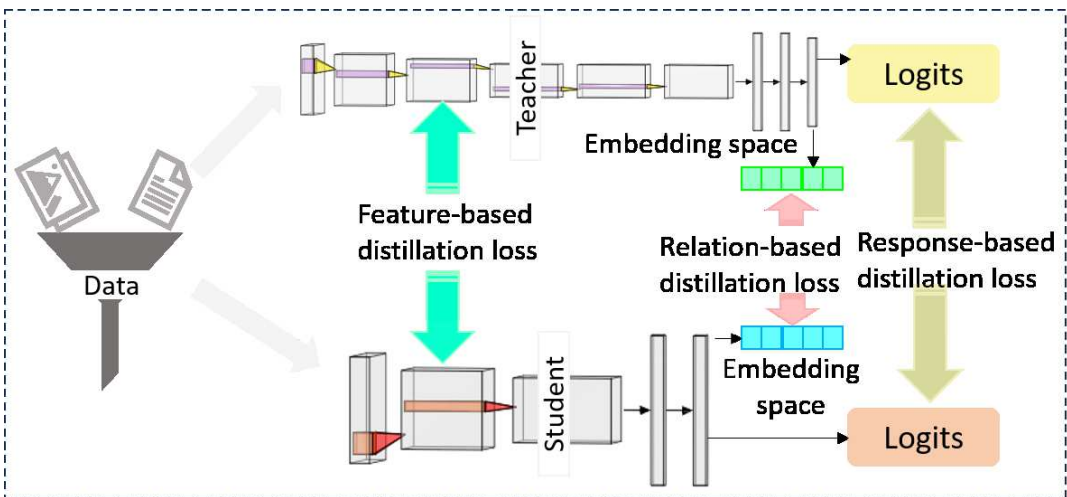


FIGURE 6 Diagrammatic representation of 1. response-based, 2. feature-based, and 3. relation-based knowledge distillation. In 1., the student mimics the teacher's soft labels. In 2., the student replicates the teacher's feature activations. In 3., the student preserves the relational structure of the teacher's data embeddings.

KD is a model compression technique in which a teacher network transfers knowledge to a smaller student network. The teacher network is typically a large neural network with many parameters. Knowledge can reside in internal layers, activations, or even soft labels 6. KD enables deployment of a smaller high-performance model on edge devices. Several studies have used KD in VLMs to enhance efficiency. [Li et al. \(2024e\)](#) introduce PromptKD, a novel approach that distills knowledge from a pretrained CLIP teacher model to a lightweight student using prompt-based imitation, enabling effective adaptation to domain-specific tasks without requiring labeled data. PromptKD additionally allows fast inference by leveraging pre-stored text features. VLMs still struggle with understanding spatial and contextual relationships. To address this SF-CLIP [Sameni et al. \(2024\)](#) employ masked knowledge distillation from pre-trained vision and language models, ensuring better spatial feature learning and multilingual retrieval while preserving training efficiency. [Fang et al. \(2021\)](#) propose a distillation approach for compressing large visual-linguistic models by aligning

student and teacher model representations. They ensure consistency in visual tokens using the same region proposals and introduce loss functions to match attention distributions and hidden states, improving efficiency without sacrificing performance. Liu et al. (2022) develop KD-VLP, an object-aware framework that embeds object-level knowledge into multimodal learning. By leveraging knowledge distillation from object features and semantic labels, their method improves cross-modal alignment and enhances downstream task performance without requiring external object detectors during inference. VLM-based detectors struggle with domain adaptation due to reliance on biased object proposals from the target domain, making direct knowledge distillation ineffective. To solve this issue, VLDadaptor Ke et al. (2024) leverage domain-mixed contrastive knowledge distillation and domain-mixed consistency distillation to align category-level features in the visual-language embedding space. Even the recent breakthrough, DeepSeek-R1 DeepSeek-AI et al. (2025), demonstrates that distilling its outputs to a student model surpasses previous non-reasoning models.

2.5 | Other Methods

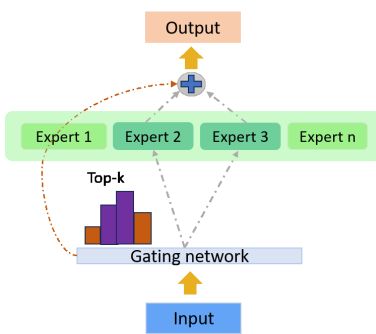


FIGURE 7 Functioning of mixture of experts (MoE) with a gating mechanism.

Recent pre-deployment work has focused on developing mixture of experts (MoE) and adaptive attention mechanisms for resource-constrained devices. Mixture of Experts enhances model efficiency by dynamically selecting specialized subnetworks or "experts," for different inputs. MoE facilitates accelerated inference relative to a model with the same number of parameters. Figure 7 shows the functioning of MoE with a gating mechanism to pass information to multiple experts. Load balancing is essential during training to avoid bias toward specific experts Wang et al. (2023b). Recent research leverages MoE to enhance efficiency in VLMs. Yu et al. (2024) introduce a parameter-efficient continuous learning framework for VLMs by integrating MoE adapters. MoE facilitates zero-shot capabilities through the dynamic selection of task-specific adapters. Shen et al. (2023) illustrate the importance of MoE in scaling VLMs while balancing the trade-off between computational resources and performance. Med-MoE Jiang et al. (2024) leverages domain-specific experts and a meta-expert to efficiently handle generative and discriminative medical tasks while reducing the number of parameters during inference. Another research focus is optimizing attention mechanisms to maintain performance while reducing FLOPs. Adaptive attention Lu et al. (2016) has emerged as a promising approach that selectively attends to tokens based on context, as compared to previous mechanisms that attended to all tokens Vaswani et al. (2017). The above described evaluation metrics and datasets are used for this as well.

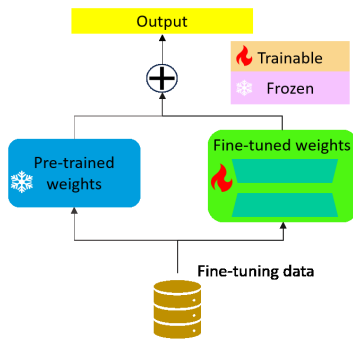
3 | EFFICIENT FINE-TUNING

Efficient fine-tuning refers to optimizing pre-trained models by updating only a small subset of parameters. Fine-tuning eliminates the need for full retraining, thereby reducing memory consumption. Fine-tuning techniques include both parameter-efficient and memory-efficient methods. The most commonly used datasets remain largely consistent with previous works, with notable additions such as MSCOCO Lin et al. (2015), MSR-VTT Xu et al. (2016), and ImageNet Deng et al. (2009). Evaluation metrics include recall@k Ji et al. (2025), harmonic mean (HM), few-shot accuracy Yao et al. (2023), and domain generalization Lu et al. (2025). Memory consumption is frequently reported to assess efficiency. Experiments are conducted on V100 and RTX 3090 GPUs.

3.1 | Parameter-Efficient Fine-Tuning (PEFT)

PEFT is a computationally efficient method for adapting neural networks by introducing a small set of trainable parameters in the last layer while keeping the remaining model's parameters and architecture unchanged. This differs from standard fine-tuning, which updates all parameters in the network. PEFT offers the following advantages: ① it reduces model size when compared to standard fine-tuning, ② mitigates the forgetting phenomenon, ③ and improves generalization to unseen contexts. PEFT includes various methods such as low-rank adaptation (LoRA), prompt tuning, adapter-based, and mapping-based approaches.

3.1.1 | Low-Rank Adaptation (LoRA)



Standard fine-tuning requires updating all model parameters, which is not only time-intensive but also requires substantial storage. In contrast, LoRA uses low-rank decomposition to approximate the weight update matrix (refer figure 8). Instead of altering the entire weight matrix $W \in \mathbb{R}^{m \times n}$, LoRA parameterizes the update matrix ΔW as the product of two lower-dimensional matrices, capturing essential task-specific adaptations. LoRA decomposes the update matrix ΔW as:

$$\Delta W = PQ^T, \quad \text{where } P \in \mathbb{R}^{m \times r}, \quad Q \in \mathbb{R}^{n \times r}. \quad (9)$$

The updated weight matrix is given by:

$$W^* = W + \Delta W = W + PQ^T. \quad (10)$$

FIGURE 8 Illustration of LoRA.

With VLMs gaining significant attention, studies have explored applying LoRA to enhance their efficiency. Bai et al. (2024) propose an adapter ensemble strategy to efficiently fine-tune large-scale VLMs while integrating LoRA to mitigate the additional parameter burden introduced by the ensemble process. By including LoRA, they aim to reduce memory and compute overhead while maintaining competitive performance, particularly in vision-language retrieval tasks. CLIP-LoRA Zanella and Ayed (2024a) reduces training overhead while maintaining strong performance across 11 datasets, demonstrating that LoRA can outperform prompt tuning and adapter-based approaches in few-shot scenarios without requiring extensive hyperparameter tuning. AdvLoRA Ji et al. (2025) builds on LoRA by introducing a parameter-efficient adversarial adaptation method for VLMs, incorporating novel reparameterization, parameter clustering, and adaptive updates to enhance both robustness and efficiency under adversarial conditions. Comp-LoRA Wang et al. (2025b) for few-shot fine-tuning of VLMs by optimizing low-rank updates in the complementary subspace, effectively mitigating catastrophic forgetting and preserving the model's original vision-language alignment capabilities. Block-LoRA Zhou et al. (2025) introduces a block matrix-based approach that partitions LoRA's low-rank matrices into sub-matrices with shared components. This leads to a reduction in the number of training parameters and simplifies computations for CLIP-based few-shot learning while retaining competitive performance. CoDyRA Lu et al. (2025) proposes a dynamic rank-selective LoRA for continual learning in VLMs, adaptively adjusting the rank of low-rank updates based on task importance. It preserves pre-trained knowledge while enabling efficient adaptation without additional inference overhead. LoRA-TTT Kojima et al. (2025) applies low-rank adaptation to the image encoder of VLMs during test time, enabling efficient domain adaptation without tuning text prompts, thereby improving generalization with minimal memory and runtime overhead. MTLoRA Agiza et al. (2024) enables efficient multi-task adaptation by using task-agnostic and task-specific low-rank modules, achieving higher accuracy with 3.6× fewer trainable parameters. Serial LoRA Zhong et al. (2025) uses a shared low-rank matrix across attention heads in vision transformers, reducing parameters to 1/4 of standard LoRA while maintaining comparable performance.

3.1.2 | Prompt Tuning

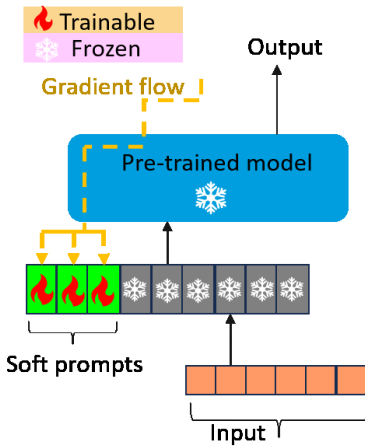


FIGURE 9 Illustration of prompt tuning.

In prompt tuning [Lester et al. \(2021\)](#), task-specific "soft prompts" are added to the input data. These are opaque learnable tensors concatenated with the input embedding as shown in figure 9. Throughout training, only the prompts are modified for the specified task. This strategy is extremely beneficial for multitasking and continual learning. [Yao et al. \(2023\)](#) introduce Knowledge-guided Context Optimization (KgCoOp) to enhance the generalization capability of prompt tuning for VLMs. Their strategy reduces the discrepancy between learned soft prompts and hard prompts, thus reducing the likelihood of forgetting important general knowledge. By integrating this optimization constraint with contrastive learning, their method improves performance on unseen classes while also maintaining computational efficiency. [Xing et al. \(2024b\)](#) propose a dual-modality prompt tuning (DPT) approach that optimizes both visual and textual prompts simultaneously to adapt vision-language models to downstream tasks. They also introduce class-aware visual prompts, generated by cross-attention between textual features and image tokens, to improve task-specific feature extraction. To address the misalignment between text and image embeddings in VLMs, [Cho et al. \(2023\)](#) develop DAPT to optimize feature distributions by maximizing inter-class separation and minimizing intra-class variability. This approach improves generalization in few-shot learning and domain adaptation.

3.1.3 | Adapter-based Transfer Learning

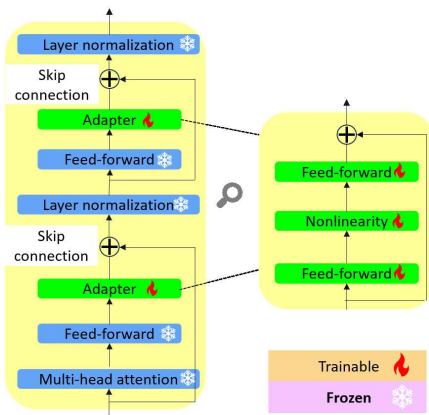


FIGURE 10 Illustration of adapters in a transformer block.

demonstrating that weight-sharing adapters achieve competitive performance with only 3.39-4.18% of updated parameters. [Yang et al. \(2024\)](#) introduce MMA (Multi-Modal Adapter) to enhance alignment between vision and language representations in VLMs by selectively integrating adapters into higher transformer layers to balance discrimination and generalization. Their approach achieves state-of-the-art performance across novel class generalization, cross-dataset adaption, and domain generalization tasks. [Cheng et al. \(2023\)](#) develop Meta-Adapter, a residual-style adapter that enables online few-shot learning for CLIP by refining features with few-shot samples to enhance generalization.

Adapter-based methods [Houlsby et al. \(2019\)](#) introduce randomly initialized bottleneck layers "A" within transformer layers, as illustrated in Figure 10. During training, adapters learn a transformation function f_A that modifies the activations of the model "h".

$$h' = f_A(h). \quad (11)$$

Adapters consist of feed-forward layers, where one layer projects the input to a lower-dimensional representation, and the other restores it to the original space. This transformation can be expressed as:

$$X \in \mathbb{R}^{a \times a} \rightarrow W_d X \in \mathbb{R}^{a \times b} \rightarrow W_u (W_d X) \in \mathbb{R}^{a \times a}. \quad (12)$$

where $W_d \in \mathbb{R}^{b \times a}$ reduces the dimension and $W_u \in \mathbb{R}^{a \times b}$ restores it. Adapters have been extensively used in large language models (LLMs) and have recently gained traction in VLMs. [Sung et al. \(2022\)](#) propose adapter-based parameter-efficient transfer learning techniques for vision and language tasks. They evaluate adapter variants in a unified multi-task setup across image-text and video-text benchmarks,

3.1.4 | Prefix Tuning

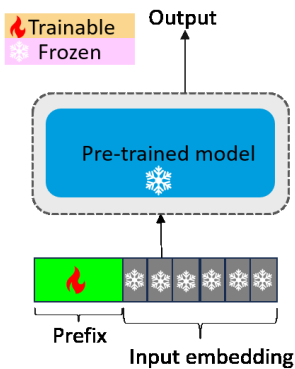


FIGURE 11 Illustration of prefix tuning.

Prefix Tuning [Li and Liang \(2021\)](#) introduces task-specific continuous vectors into each layer of the transformer architecture. Prefixes are abstract representations concatenated with input embeddings in each layer. These vectors are optimized during fine-tuning and act as soft prompts that steer the model toward task-specific behavior without updating the backbone parameters. [van Sonsbeek et al. \(2023\)](#) introduce a mapping network that transforms visual features into token embeddings and employs prefix tuning to refine query representations in each transformer layer for open-ended medical visual question answering (VQA). [Song et al. \(2024b\)](#) propose a vision-language storytelling framework that integrates a trainable transformer mapping network and a multimodal contrastive objective to enhance coherence in generated narratives. Prefix tuning is employed to align CLIP-extracted visual features with a frozen GPT-2 [Radford et al. \(2019\)](#) model, facilitating efficient vision-language alignment. Prefixes are introduced in personalized image captioning to map visual features with user context, enabling a frozen GPT-2 model to provide personalized captions [Wang et al. \(2023c\)](#).

3.2 | Memory-Efficient Fine-Tuning (MEFT)

Memory-Efficient Fine-Tuning (MEFT) [Liao et al. \(2023\)](#) optimizes large pre-trained models for downstream tasks while minimizing memory overhead. Unlike traditional fine-tuning, which involves backpropagation through the entire model, MEFT reduces activation storage and memory-intensive gradient computations. One such method, LoSA [Mercea et al. \(2024\)](#) avoids backpropagation through the backbone. This is achieved by incorporating a lightweight parallel network that refines features from the backbone. Transformer models remain integral to VLMs, making MEFT-based optimization crucial for efficient fine-tuning across diverse applications. One such method is SLIMFIT [Ardakani et al. \(2024\)](#), which dynamically freezes less-contributory layers based on training dynamics and combines this with quantization and pruning to reduce activation memory. This method saves up to 3.1× on-device memory and maintains accuracy within 0.4% of full fine-tuning. [Liu et al. \(2024a\)](#) develop M^2IST (Multi-Modal Interactive Side-Tuning) to enhance vision-language alignment and enable memory-efficient fine-tuning (MEFT) for referring expression comprehension (REC). By freezing pre-trained encoders and updating lightweight side networks, M^2IST reduces GPU memory usage by 60.39% compared to full fine-tuning.

4 | RUNTIME OPTIMIZATIONS

Runtime optimization refers to techniques that dynamically adjust computations during inference to improve computational efficiency, memory use, and energy consumption without requiring retraining. Unlike static optimizations such as pruning or quantization, runtime methods adapt model execution on-the-fly based on input complexity, hardware constraints, or task-specific requirements. VLMs are computationally intensive, necessitating significant processing for multimodal interactions. Their deployment on resource-constrained devices is challenging due to the high memory, power, and latency demands. Runtime optimization mitigates these issues by reducing unnecessary computations and accelerating inference. The datasets evaluated remain consistent with those in previous sections, with top-k accuracy [Farina et al. \(2024a\)](#); [MA et al. \(2023\)](#) being the primary evaluation metric. GPU consumption is also lower when compared to other techniques previously described, as computations are adjusted dynamically during inference.

4.1 | Token Reduction

A major bottleneck in VLMs is redundant token processing, particularly in transformer-based models where both visual and textual tokens contribute to high computational costs. Since VLMs compute relationships between all visual tokens (N_v) and textual tokens (N_t) using cross-attention mechanisms, the computational complexity grows quadratically as $O(N_v \times N_t)$, leading to significant inefficiencies during multi-modal fusion. Token reduction dynamically prunes, merges, or selectively processes tokens at inference time to optimize speed and memory usage. PuMer dynamically removes redundant tokens and merges similar ones in both vision and language modalities during inference [Cao et al. \(2023\)](#). Unlike pre-deployment pruning, PuMer adapts token selection per instance to improve efficiency while maintaining performance. Turbo [Ju et al. \(2024\)](#) employs mutual redundancy and semantic value-based token pruning, using an informativity score to rank tokens. This score evaluates redundancy and contribution to semantics, enabling Turbo to delete less informative tokens while retaining crucial ones. This method enhances inference speed and reduces computational overhead in VLMs.

4.2 | Test-Time Adaptation (TTA)

TTA dynamically adjusts inference strategies in real-time without modifying model weights, allowing models to adapt to domain shifts and unseen data. Unlike traditional fine-tuning, TTA operates on-the-fly during inference. Standard VLMs process inputs using a fixed learned distribution $p(y | x; \theta)$, but in real-world settings, the input distribution $p(x)$ often shifts. This causes performance degradation. TTA mitigates this by estimating an updated conditional probability:

$$p(y | x) = \operatorname{argmax}_y \mathbb{E}_{q(\theta)} [p(y | x; \theta)]. \quad (13)$$

where $q(\theta)$ represents an adapted inference distribution that dynamically adjusts based on observed data. [MA et al. \(2023\)](#) introduce SwapPrompt, a contrastive learning-based approach that dynamically adjusts prompts during inference to improve zero-shot classification by aligning textual representations with appropriate visual features. [Fuchs et al. \(2025\)](#) develop OGA (Online Gaussian Adaptation), a TTA method for VLMs that models visual feature likelihoods using multivariate Gaussian distributions. By incorporating zero-shot priors into a MAP (Maximum A Posteriori) framework, OGA improves robustness without the need for dataset-specific hyperparameter tuning. TDA (Training-free Dynamic Adapter) [Karmanov et al. \(2024a\)](#) maintains a key-value cache for pseudo labels and test sample features, enabling progressive adaptation without backpropagation. This significantly reduces computational overhead. [Farina et al. \(2024a\)](#) introduce ZERO, a test-time adaptation method that improves VLM robustness without optimization. It marginalizes over augmented views and applies a zero-temperature Softmax, achieving state-of-the-art results while being 10× faster and 13× more memory efficient than test-time prompt tuning. We provide details on TTA techniques in [4.2.1](#) and [4.2.2](#).

4.2.1 | Test-Time Augmentation

Test-time augmentation involves applying various transformations to test data and aggregating the model's predictions to enhance performance during inference. By leveraging multiple augmented versions, test-time augmentation improves accuracy without the need for retraining, making it well-suited for low-power inference scenarios. MTA (Mean-Shift for Test-time Augmentation) [Zanella and Ayed \(2024b\)](#) enhances zero-shot generalization of VLMs by leveraging multiple augmented views without requiring prompt tuning or model retraining. It filters augmented views using in-lierness assessment and refines embeddings with robust MeanShift optimization. MTA is $\approx 3\times$ faster than the prompt tuning method in computation time. Unlike standard test-time augmentation, [Kimura and Bondell \(2024\)](#) use variational Bayes to weight augmentations, suppressing ineffective ones for better predictions. CutMixOut [Fawakherji et al. \(2024\)](#) introduces a novel test-time text augmentation approach for multimodal person re-identification. It applies CutMix and CutOut to text descriptions during inference to improve retrieval accuracy without the need for additional training.

4.2.2 | Test-Time Prompt Tuning (TPT)

TPT optimizes prompts at inference time to enhance the generalization of frozen VLMs. Given a test sample x_t , the goal is to adjust the prompt representation p_t such that the similarity between the test image feature $f_v(x_t)$ and the optimized text feature $f_t(p_t)$ is maximized:

$$p_t^* = \operatorname{argmax}_{p_t} \cos(f_v(x_t), f_t(p_t)). \quad (14)$$

where $f_v(x_t)$ is the visual feature extracted by the vision encoder and $f_t(p_t)$ is the text feature from the language encoder. TPT [Manli et al. \(2022\)](#) optimizes prompts using entropy minimization across augmented views, enhancing zero-shot top-1 accuracy of CLIP by an average of 3.6%. C-TPT [Yoon et al. \(2024\)](#) improves TPT by using text feature dispersion to enhance calibration while preserving accuracy, achieving better uncertainty quantification without labeled data. Self-TPT [Zhu et al. \(2024\)](#) further improves TPT with self-supervised learning, achieving strong performance with 25× faster inference and 30× lower memory use.

We compare the various paradigms and techniques for engineering efficient VLMs in Table 2. The summary provides an overview of the computational efficiency and memory requirements of the methods described in sections two through four and the best use cases for each technique. Pre-deployment techniques give the best efficiency in terms of inference time and storage because they shrink the model before deployment, leading to a smaller model on the disk. Efficient fine-tuning techniques do not speed up inference nor reduce storage because they leave the entire model intact and only add adapters or prompts. Runtime optimizations eliminate redundant inference computations to deliver some speedup while preserving the majority of model parameters.

TABLE 2 Comparison of computational efficiency and memory requirement across various techniques. ● indicates best performance; ● indicates medium performance; ● indicates worst performance.

Paradigm	Technique	Compute Efficiency	Memory Requirements	Use Case
Pre-Deployment	Post-Training Quantization	●	●	Reduce model size and improve latency at deployment. Useful to deploy on low-memory devices at the cost of accuracy.
	Structured Pruning	●	●	Remove redundant weights for sparse model deployment. Useful if CPU/GPU supports sparse matrix ops.
	Knowledge Distillation	●	●	Train a smaller student for fast, lightweight inference. Useful for application specific deployment
Efficient Fine-Tuning	Low-Rank Adaptation (LoRA)	●	●	Low-resource fine-tuning without changing base weights. Requires server to fine-tune the model
	Prompt Tuning	●	●	Efficient task adaptation with minimal updates. Requires server to fine-tune the model unless on tiny VLMs
	Adapter based Transfer Learning	●	●	Reusable modules across tasks without retraining full model.
Runtime Optimization	Token Reduction	●	●	Speed up inference by processing fewer tokens.
	Test-Time Adaptation	●	●	Dynamically adapt to domain shifts or out-of-distribution data.
	Test-Time Prompt Tuning	●	●	Apply small prompts at runtime for improved generalization.

5 | PRIVACY-PRESERVING DISTRIBUTED VLM

Privacy-preserving distributed VLM ensures that model training occurs across multiple devices or servers without sharing raw data. The key benefits include enhanced data security and a decreased risk of data leakage. The datasets and evaluation metrics used remain the same as in previous sections. However, computational resources differ depending on the client devices. For instance, a Jetson Nano has 4GB RAM, while a Jetson Orin offers 8GB RAM, reflecting one example of such variation. Below, we discuss key techniques such as Federated Learning (FL) 5.1 and Split Learning 5.2.

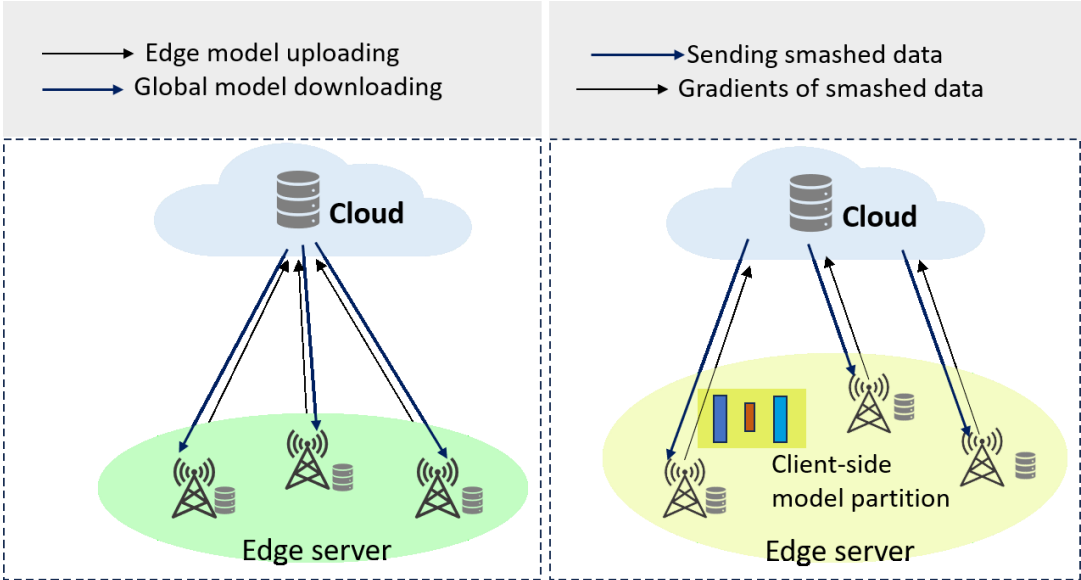


FIGURE 12 (left) Working of federated learning and (right) split learning.

5.1 | Federated Learning (FL)

FL (figure 12 (left)) allows multiple clients $\langle C_1, C_2, \dots, C_N \rangle$ to collaboratively update a global model w without sharing raw data. Each client updates w by minimizing a local loss function L_i using its data D_i , and sends only model updates Δw_i to a central aggregator. The global model (usually a server model) is then updated using techniques such as FedAvg McMahan et al. (2016) and FedProx Zheng et al. (2021). Recently, several studies have explored FL with VLMs Pan et al. (2024); Zeng et al. (2024). PMG-FL (personalized and multi-granularity federated learning) Gao et al. (2024a) efficiently adapts vision-language foundation models on edge devices, addressing challenges such as data heterogeneity and limited resource availability through prompt-based local adaptation and knowledge fusion across different device granularities. Yan and Guo (2024) introduce a lightweight unsupervised federated learning framework (FST-CBDG) that leverages pre-trained VLMs to enhance model adaptation on edge devices without requiring labeled data. By refining pseudo-labels through self-training and addressing data heterogeneity with class-balanced data generation, this approach significantly reduces computational and communication overhead. pFedPrompt Guo et al. (2023) improves personalization in FL by adapting the prompts to user-specific data and using multimodal learning for efficient model alignment.

5.2 | Split Learning

Split Learning (figure 12 (right)) is a distributed learning technique where a deep model is split between clients and a central server, enabling collaborative training without sharing raw data. Split Learning ensures privacy by partitioning the model into client-side $f_c(\theta_c)$ and server-side $f_s(\theta_s)$, where θ_c and θ_s represent the parameters of the client and server models, respectively. Instead of transmitting raw data x , the client sends only intermediate activations $h = f_c(x; \theta_c)$ to the server. The server then processes h using $f_s(\theta_s)$, ensuring that sensitive data remains local while enabling collaborative model optimization. Although direct applications of split learning to VLMs are scarce, related works provide useful insights. For example, SplitLoRA Lin et al. (2024b) has been explored for large language models (LLMs), which often serve as the language encoder in VLMs. Similarly, Bidirectional Contrastive Split Learning Sun and Ochiai (2024) has been applied for a VQA task, demonstrating split learning's potential in multimodal settings.

6 | LIGHTWEIGHT VISION-LANGUAGE MODELS

The need for efficiency, scalability, and deployment on resource-constrained devices has driven the transition from large-parameter VLMs to lightweight models. Smaller VLMs optimize architecture and tokenization to maintain strong multimodal performance while reducing memory, latency, and energy costs. Lightweight models usually reduce the number of parameters using techniques or a combination of techniques described above. Figure 13 compares model parameters between some lightweight and large-scale VLMs.

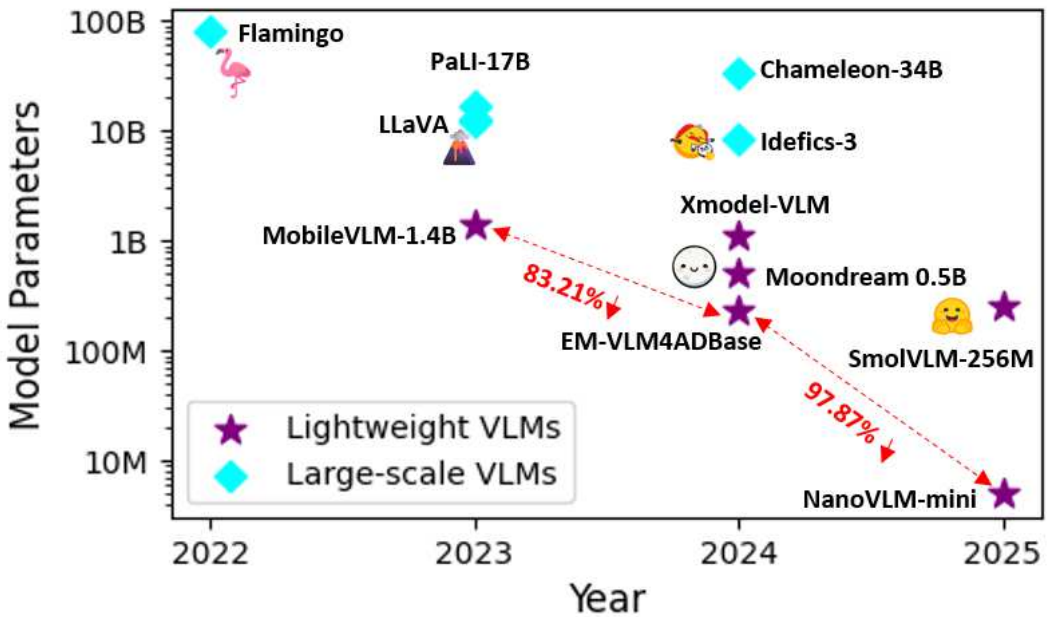


FIGURE 13 Parameter distribution of some lightweight and large-scale VLMs over time. Recent years have witnessed a growing emphasis on lightweight VLMs.

6.1 | SmolVLM

SmolVLM-256M and SmolVLM-500M [Marafioti et al. \(2025\)](#) are the latest additions to the lightweight VLM family. SmolVLM-256M performs well in captioning, document Q&A, and basic visual reasoning tasks. SmolVLM-500M offers notable performance gains over its sibling while remaining lightweight. The latest models achieve this efficiency by replacing the SigLIP 400M SO vision encoder with the SigLIP base patch-16/512 (93M).

6.2 | MobileVLM

MobileVLM [Chu et al. \(2023\)](#) is a high-performance, mobile-scale VLM designed for efficient deployment on resource-constrained devices. It introduces MobileLLaMA (1.4B & 2.7B parameters), along with an optimized vision encoder and a lightweight downsample projector (LDP) for efficient visual-text alignment. MobileVLM offers strong multimodal performance on various benchmarks while maintaining low latency, with 21.5 tokens/s on Snapdragon 888 CPU and 65.3 tokens/s on Jetson Orin GPU.

6.3 | EM-VLM4AD

EM-VLM4AD [Gopalkrishnan et al. \(2024\)](#) is a lightweight VLM developed for VQA in autonomous driving. It efficiently processes multi-view traffic scene images using gated pooling attention to extract relevant spatial information. The model features two lightweight language backbones: a fine-tuned T5-Base (235M parameters) and an 8-bit quantized T5-Large (769M parameters), significantly reducing memory (up to 10x) and FLOP requirements compared to prior VLMs.

6.4 | EfficientVLM

EfficientVLM [Wang et al. \(2023a\)](#) is a fast and compact VLM that reduces parameter count to 93M (44.3% of the teacher model) while retaining 98.4% performance and accelerating inference by 2.2x. This is achieved by a distillation then pruning approach, wherein knowledge distillation compresses the model while maintaining accuracy, and modal-adaptive pruning selectively eliminates redundant structures in vision and language encoders according to task importance.

6.5 | MiniVLM

MiniVLM [Wang et al. \(2021\)](#) is a lightweight VLM that reduces parameters to 27% and FLOPs to 1% of OSCAR [Li et al. \(2020\)](#) while retaining 94–97% accuracy. This makes MiniVLM optimal for resource-constrained deployments. It achieves this via TEE (Two-stage Efficient feature Extractor) for faster visual processing and a MiniLM-based transformer for vision-language fusion.

6.6 | LightCLIP

LightCLIP [Nie et al. \(2023\)](#) enhances efficiency with three key techniques: ① progressive label softening for better instance alignment, ② bipartite matching for fine-grained image-text alignment, ③ and MLM with image-text fusion to optimize a compact text encoder. It significantly improves zero-shot classification and retrieval performance without increasing inference costs, making it useful for resource-constrained environments.

TABLE 3 Comparison of **frameworks** & **libraries** for VLM optimization, fine-tuning, edge execution, and FL integration. ✓ indicates support, ✗ indicates no support, and ◐ indicates partial support.

Framework / Library	Optimization Techniques Supported	Fine-Tuning Techniques Supported	Edge Execution	Supported VLM Models	Federated Learning Support
EdgeVL Cai et al. (2024)	Dual-modality knowledge distillation, quantization-aware training	Fine-tuning via contrastive learning and distillation	✓	Adapted CLIP-based VLMs for edge deployment	✗
DeepSpeed ¹	Zero and sparse training optimizations	Distributed fine-tuning and model parallelism	✓	Large VLMs (e.g., LLaVA variants, Flamingo, MiniGPT-4, etc.)	Not directly (requires custom FL loop on top of DeepSpeed modules)
Hugging Face Transformers ² + Optimum ³	Quantization (INT8/FP16), pruning, distillation	Full fine-tuning, LoRA, adapters, prompt tuning	✓	CLIP, BLIP, ViLT, VisualBERT, FLAVA, LLaVA variants (e.g., LLaVA, LLaVA 1.5, LLaVA 1.6, LLaVA-CoT, LLaVA-Plus, u-LLaVA, etc.)	◐
TensorRT-LLM ⁴	INT8 & FP16 quantization, layer fusion	Inference-only (no native fine-tuning)	✓	Converted models (e.g., CLIP, BLIP, MobileVLM)	✗
OpenVINO (with NNCF) ⁵	Post-training quantization, structured pruning, sparsity	Limited transfer learning via model conversion	✓	CLIP, custom compact VLMs (e.g., MiniVLM ports)	✗
Apache TVM ⁶	Quantization and pruning	Primarily a compiler/optimization tool	✓	Any exportable VLM (e.g., CLIP, BLIP, Flamingo variants)	✗
ONNX Runtime ⁷	Graph optimizations, quantization	Emerging support for ONNX training (minimal fine-tuning)	✓	VLMs (e.g., CLIP, BLIP, MobileVLM, LLaVA variants)	✗
NVIDIA TAO Toolkit ⁸	Quantization, pruning, distillation	Transfer learning with parameter-efficient methods (e.g., adapters)	✓	NVIDIA-optimized models (e.g., MobileVLM V2, Moondream2)	✗
NVIDIA Triton Inference Server ⁹	Graph optimizations, quantization, runtime optimizations	N/A (serves for inference, not fine-tuning)	✓	VLMs (e.g., CLIP, BLIP, MobileVLM, LLaVA variants)	✗
FedML ¹⁰	Via integration with standard compression libraries	Federated fine-tuning, including parameter-efficient approaches	✓	Custom VLMs (e.g., CLIP variants) via federated training	✓
PySyft ²	Can be integrated with standard compression techniques	Federated fine-tuning with secure aggregation	✓	Custom PyTorch-based VLMs (e.g., CLIP, BLIP, LLaVA variants)	✓

6.7 | NanoVLMs

NanoVLMs [Agarwalla et al. \(2025\)](#) introduce ultra-small VLMs (5M, 16M, & 25M parameters) optimized for efficiency. NanoVLMs prioritize better parameter allocation across a compact visual encoder, a lightweight language decoder, and a simple visual-text connector. The novelty lies in scaling down VLMs without sacrificing coherence or fluency.

6.8 | Moondream

Moondream AI 2B (1.9B parameters) supports fp16, int8, and int4 quantization for efficient GPU and CPU inference on mobile devices. Moondream 0.5B (0.5B parameters) uses int8 and int4 quantization and is optimized for mobile and edge devices. Both models use QAT (refer to section 2.1.2) to enhance efficiency.

6.9 | Xmodel-VLM

Xmodel-VLM [Xu et al. \(2024\)](#) is a 1B-scale lightweight VLM which uses CLIP ViT-L/14@336 for vision, Xmodel-LM-1B for language, and an XDP projector for reduced visual tokens. Following the LLaVA paradigm, it goes through two stages of training for feature alignment and instruction tuning. Despite being small, it delivers competitive performance on multimodal benchmarks while maintaining low inference latency.

Furthermore, Table 3 outlines various frameworks and libraries. This table provides readers and researchers with a comprehensive overview of each library/framework’s capabilities to help them choose the right tool. Table 4 summarizes the parameter counts, methodologies, and advantages of various compact VLMs. Although larger models often correlate with better performance, the primary intent of this table is to highlight that models with significantly fewer parameters (often in the low million range) can still outperform baseline models while offering benefits in speed and memory efficiency. This performance gain stems largely from selecting the most appropriate method for the task. For example, rows 1–3 demonstrate that techniques like LoRA and knowledge distillation enable competitive or superior

TABLE 4 Efficient models with parameter size, methods used, and advantages.

Model/Method Name	Parameters	Method(s)	Advantage
CLIP-LoRA Zanella and Ayed (2024a)	149M total / ~16M trainable	LoRA on query, key, value matrices of both vision and text encoders (rank=2).	Outperforms or matches full fine-tuning performance across 11 few-shot classification datasets.
PromptKD Li et al. (2024e)	≈ 340M (student)	Prompt-based distillation using pre-stored class vectors and KL alignment of image logits with teacher CLIP.	Improves zero-shot accuracy by 12% (HM) over CLIP across 11 datasets.
KD-VLP Liu et al. (2022)	≈ 138M (student)	Object-guided masked vision modeling & phrase-region alignment using knowledge distillation from external object detectors.	Achieves comparable retrieval and reasoning performance with significantly fewer parameters.
LoRA-Sparse Song et al. (2024a)	≈ 600M (upper bound estimate of trainable parameters)	Applies low-rank linear projection layers for sparse attention approximation.	Maintains baseline accuracy with 70% fewer trainable parameters.
MedVILL Moon et al. (2022)	≈ 110M	Joint masked language modeling & image-report alignment using BERT with multimodal attention masking.	Outperforms baselines on both VLU and VLG tasks with strong generalization to unseen data.
TDA Karmanov et al. (2024a)	≈ 102M (RN50) / ≈ 149M (ViT-B/16); doesn't add trainable weights beyond CLIP	Training-free dynamic adapter using dual key-value caches for efficient test-time adaptation of CLIP.	Achieves +1.54% accuracy gain over baseline CLIP while reducing test time to just 16 minutes without backpropagation.
FastVLM Vasu et al. (2025)	125M (vision) + LLM (e.g. 0.5B / 1.2B / 7B)	Combines a hybrid FastViTHD encoder with reduced visual tokens for efficient high-resolution vision-language modeling.	Achieves 3.2x improvement in time-to-first-token (TTFT) while maintaining similar performance on VLM benchmarks.
VisualBERT Li et al. (2019)	110M	Jointly embeds text and object-level image features using a unified Transformer with visually-grounded pretraining on caption data.	Outperforms Pythia baselines on VQA with 70.80% (Test-Dev) and 71.00% (Test-Std) accuracy using a simpler architecture.

performance with substantial reductions in parameter size. However, these techniques depend heavily on the objectives: For instance, Knowledge distillation yields compact student models but sacrifices the teacher's representational richness, rendering them more suitable for specialized tasks than for multitask scenarios. Fine-tuning techniques such as LoRA are chosen for efficient adaptation with minimal additional parameters, while pre-deployment techniques such as knowledge distillation is used to transfer a large model's full predictive behavior into a compact student network. This table demonstrates how various techniques described above yield compact VLMs that match or exceed baseline performance with far fewer parameters, while detailing their specific methods.

7 | ANALYSIS AND INSIGHTS

In this section, we ① analyze the impact of efficiency-driven techniques on accuracy, latency, and memory usage, and ② present the performance of several VLMs across various multimodal benchmarks.

7.1 | Impact of Efficiency-Boosting Techniques on Accuracy, Memory, and Latency

Our evaluation is based on two models: ① *blip-vqa-base* [Li et al. \(2022a\)](#) (~385M parameters) and ② *vilt-b32-finetuned-vqa* [Kim et al. \(2021\)](#) (~87M parameters). All results are reported using an NVIDIA RTX A6000 GPU. We use the Balanced Binary Abstract Scenes [Zhang et al. \(2016\)](#) dataset which is a visual question answering (VQA) dataset, where each sample consists of an abstract scene image, a natural language question, and multiple human-annotated answers. Evaluation is based on the official VQA accuracy metric, which grants full credit if at least three out of ten annotators provide the same answer as the model. We also measure average inference latency and memory consumption to assess runtime efficiency. Notably, the observed trends remain consistent across all models, provided the parameter count falls within the range of these two models. This section provides insights specifically for pre-deployment techniques such as quantization, pruning, and low-rank approximation. We focus on these methods because they are fundamental for optimizing models before deployment, directly impacting model size and performance. Although efficient fine-tuning, runtime optimizations, and privacy-preserving methods are important, they are often model- or task-specific and involve different challenges and considerations that extend beyond the scope of this survey. Our analysis provides insights into the

accuracy vs. efficiency trade-off, and emphasizes the importance of selecting the right technique.

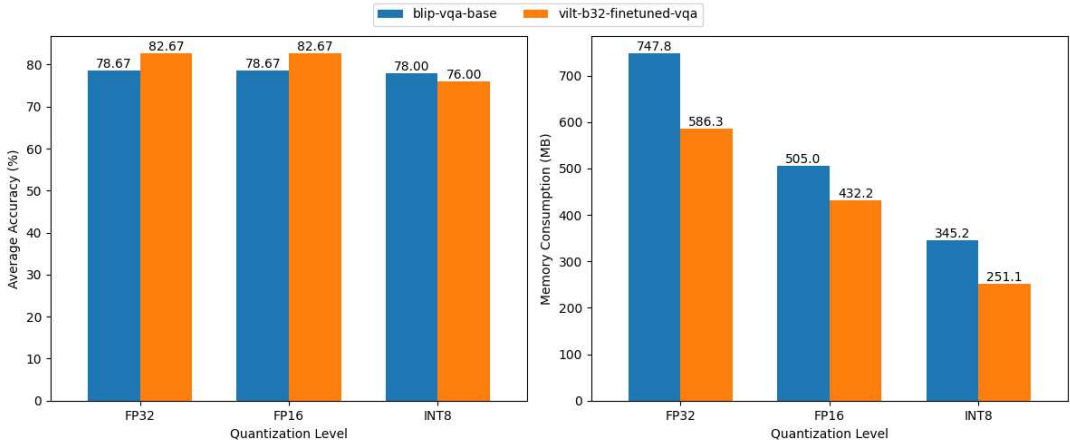


FIGURE 14 (Left) Average accuracy for FP32, FP16, and INT8 quantization across 50 samples. (Right) Corresponding memory consumption.

We conducted FP16 inference on GPU with `torch.amp.autocast` and INT8 inference using dynamic quantization of linear layers. Quantization (figure 14) has a notable impact on accuracy, latency, and memory consumption on both `blip-vqa-base` and `vilt-b32-finetuned-vqa`. For `blip-vqa-base`, transitioning from FP32 to INT8 results in a 0.85% accuracy drop for 50 samples whereas `vilt-b32-finetuned-vqa` experiences an 8.07% reduction indicating that ViLT is more sensitive to INT8 quantization. We also increase the number of samples to 125 to observe the effect on accuracy and memory consumption. Increasing the sample size from 50 to 125 causes a 1.36% accuracy drop in FP32 and a 1.54% drop in INT8 for `blip-vqa-base`, while `vilt-b32-finetuned-vqa` sees a 7.1% decrease in FP32 and a 0.09% reduction in INT8. However, the accuracy drop for `vilt-b32-finetuned-vqa` from FP32 to INT8 is steeper (4.6% on average) compared to `blip-vqa-base` (0.94%), suggesting that `vilt-b32-finetuned-vqa` benefits more from higher precision, but suffers greater degradation from aggressive quantization. In terms of memory consumption, quantization significantly reduces memory requirements across both models. For `blip-vqa-base`, moving from FP32 to INT8 results in a 53.8% reduction (747.8MB to 345.2MB) for 50 samples and a 43.1% reduction (800MB to 455MB) for 125 samples, while `vilt-b32-finetuned-vqa` achieves a 57.2% reduction (586.3MB to 251.1MB) for 50 samples and 44.2% (664.4MB to 370.6MB) for 125 samples, demonstrating that INT8 provides substantial memory savings, with `vilt-b32-finetuned-vqa` benefiting slightly more. Across all quantization levels, `blip-vqa-base` consistently consumes more memory than `vilt-b32-finetuned-vqa`, with a difference of 161.5MB in FP32 (50 samples) and 94.1MB in INT8 (50 samples). The `blip-vqa-base` maintains a more stable accuracy across sample sizes but consistently requires more memory. The latency per sample remains 0.0877s, 0.0757s, and 0.0701s across FP32, FP16, and INT8 for `blip-vqa-base` and 0.0330s, 0.0321s, and 0.0311s for `vilt-b32-finetuned-vqa`, with INT8 being the fastest in both cases. For FP32, we run the models with full 32-bit precision. For

¹<https://www.deepspeed.ai/>

²<https://github.com/OpenMined/PySyft>

³<https://huggingface.co/docs/optimum/>

⁴<https://developer.nvidia.com/tensorrt>

⁵<https://docs.openvino.ai/2025/index.html>

⁶<https://tvm.apache.org/>

⁷<https://github.com/microsoft/onnxruntime>

⁸<https://developer.nvidia.com/tao-toolkit>

⁹<https://github.com/triton-inference-server/server>

¹⁰<https://fedml.ai/>

FP16, mixed precision is enabled using autocasting to boost speed while maintaining accuracy. For INT8, a copy is dynamically quantized on its linear layers to shrink the model and speed up inference.

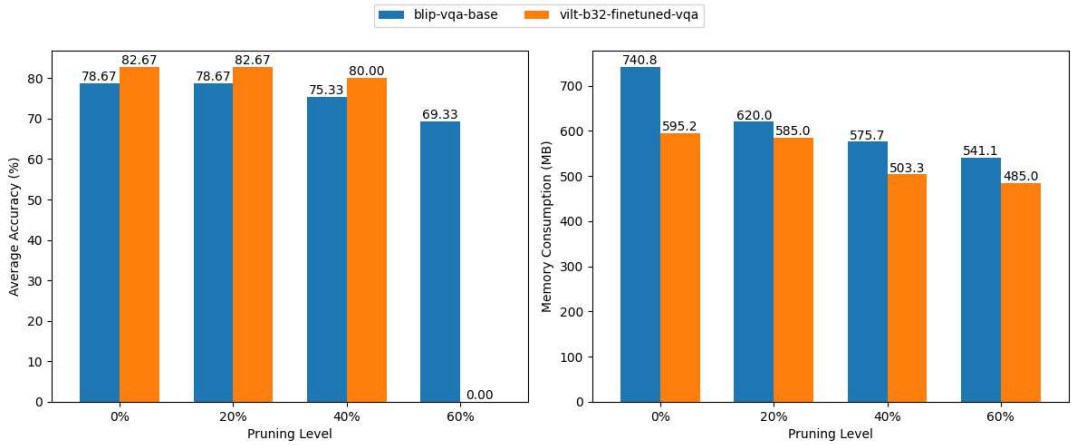


FIGURE 15 (Left) Average accuracy for 0%, 20%, 40% and 60% pruning across 50 samples. (Right) Corresponding memory consumption.

We applied global unstructured L1 pruning to all linear layers at 20%, 40%, and 60% sparsity to evaluate the impact of weight sparsification. Pruning (figure 15) significantly impacts accuracy and memory consumption across both models. For blip-vqa-base, accuracy drops by 0% at 20% pruning, 4.24% at 40% pruning and 11.9% at 60% pruning for 50 samples. The vilt-b32-finetuned-vqa model follows a similar trend, but at 60% pruning, accuracy drops to 0%, indicating extreme sensitivity to high sparsity levels. In terms of memory savings, blip-vqa-base reduces by 16.3% at 20% pruning, 22.3% at 40% pruning, and 27% at 60% pruning (50 samples), while vilt-b32-finetuned-vqa achieves reductions of 1.7%, 15.4%, and 18.5%, respectively. For 125 samples, blip-vqa-base saves 12.3%, 20.7%, and 24.9%, whereas vilt-b32-finetuned-vqa reduces by 4.2%, 13.4%, and 21%. The results show that vilt-b32-finetuned-vqa maintains better accuracy at lower pruning levels but is highly sensitive to aggressive pruning. The latency per sample for blip-vqa-base at 20%, 40%, and 60% pruning is 0.0569s, 0.0561s, and 0.0559s, respectively, while for vilt-b32-finetuned-vqa, it is 0.0148s, 0.0141s, and 0.0139s at the same pruning levels. We observe that pruning results in faster inference per sample compared to quantization. We implement pruning by scanning all model modules to find linear layers and then apply global unstructured L1 pruning with a set sparsity ratio. After pruning, the extra reparameterization is removed, making the pruned model ready for inference.

We applied low-rank approximation to every linear layer by truncating singular values at rank ratios of 0.8, 0.6, and 0.4. Low-rank approximation (figure 16) significantly affects accuracy and memory consumption across both models. Decreasing the rank from $k = 0.8$ to $k = 0.4$ increases compression, leading to lower memory consumption and latency. However, this also results in a drop in accuracy. For blip-vqa-base, accuracy decreases by 15.8% at $k = 0.8$, 27.8% at $k = 0.6$, and drops to 0% at $k = 0.4$ for 50 samples. The vilt-b32-finetuned-vqa exhibits a more gradual decline, with accuracy dropping by 4% at $k = 0.8$, 6.2% at $k = 0.6$, and 27.1% at $k = 0.4$, indicating that vilt-b32-finetuned-vqa is more resilient to LRA compared to blip-vqa-base. In terms of memory savings, blip-vqa-base reduces memory consumption by 140 MB at $k = 0.8$, 160.7 MB at $k = 0.6$, and 208.6 MB at $k = 0.4$ (50 samples), while vilt-b32-finetuned-vqa achieves reductions of 7.2 MB, 63.2 MB, and 86.4 MB, respectively. For 125 samples, blip-vqa-base saves 65.4 MB, 100.2 MB, and 199.3 MB, whereas vilt-b32-finetuned-vqa reduces by 64 MB, 83.8 MB, and 150 MB. This indicates that while low-rank approximation provides substantial memory savings, blip-vqa-base is highly sensitive to aggressive rank reduction, whereas vilt-b32-finetuned-vqa maintains better accuracy at even lower ranks. The latency per sample for blip-vqa-base at $k = 0.8$, $k = 0.6$, and $k = 0.4$ is 0.0442s, 0.0435s, and 0.0429s, respectively, while for vilt-b32-finetuned-vqa, it

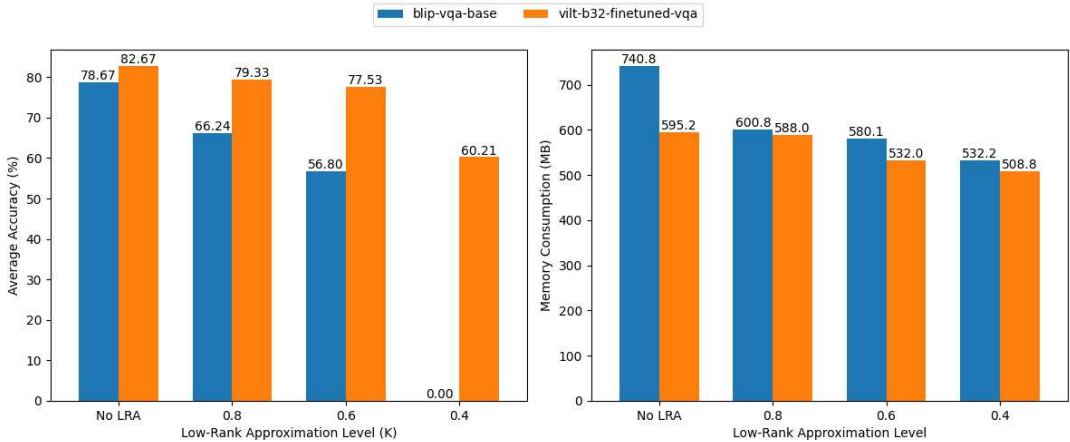


FIGURE 16 (Left) Average accuracy for no low-rank approximation, $k = 0.8$, $k = 0.6$, and $k = 0.4$ across 50 samples. (Right) Corresponding memory consumption.

is 0.0148s, 0.0136s, and 0.0136s at the same rank reduction levels. We observe that low-rank approximation leads to lower latency per sample compared to quantization and pruning. We implement low-rank approximation by iterating over each linear layer, computing a reduced rank from a given ratio, and performing SVD on the weight matrix. Only the top singular values and vectors are kept to reconstruct an approximated weight, which replaces the original.

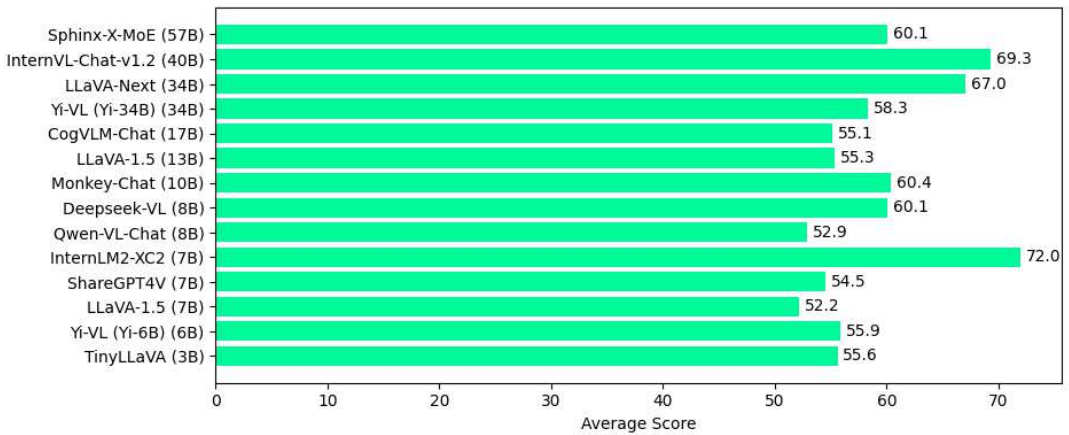


FIGURE 17 Evaluation of various VLMs across multiple multimodal benchmarks, including MMMU [Yue et al. \(2024a\)](#), MMB [Liu et al. \(2023a\)](#), ScienceQA [Lu et al. \(2022\)](#), AI2D [Kembhavi et al. \(2016\)](#), SEED [Li et al. \(2023\)](#), and MathVista [Lu et al. \(2024\)](#). The average score represents the mean performance across all benchmarks. Data for this plot is sourced from [Chen et al. \(2024a\)](#).

7.2 | Evaluating VLM Performance on Benchmark Multimodal Datasets

We present the performance of various VLMs with differing parameter counts across widely used benchmarks to enable comparative analysis. Figure 17 illustrates the average scores of 14 different VLMs evaluated on 6 multimodal benchmarks. **The average score is depicted in the figure.** Interestingly, the results show that a higher parameter count does not necessarily translate to better accuracy. For example, InternLM2-XC2, with 7B parameters, achieves an impressive average score of 72, while Sphinx-X-MoE, despite having 57B parameters, achieves a lower average score of

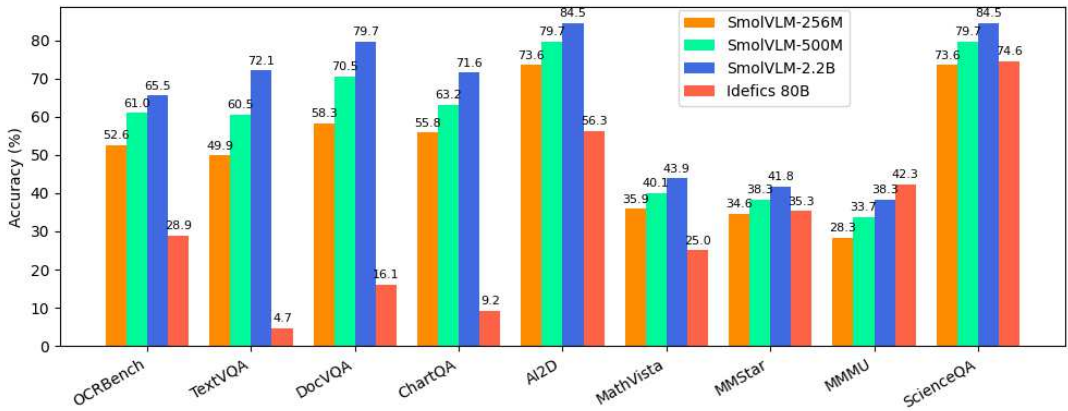


FIGURE 18 Evaluation of VLMs of varying sizes (256M, 500M, 2.2B, and 80B) across multiple multimodal benchmarks, including OCRBench Liu et al. (2024b), TextVQA Singh et al. (2019), DocVQA Mathew et al. (2021), ChartQA Masry et al. (2022), AI2D Kembhavi et al. (2016), MathVista Lu et al. (2024), MMStar Chen et al. (2024a), MMMU Yue et al. (2024a), and ScienceQA Lu et al. (2022). Data for this plot is sourced from <https://huggingface.co/blog/smolervlm>

just 60.1. Similarly, comparatively smaller models like TinyLLaVA and Yi-VL, with 3B and 6B parameters respectively, achieve competitive average scores around 56. These findings suggest that the performance of a VLM depends more on the optimization method and design choices than on model size alone, which is an important insight for selecting or designing models suitable for deployment on edge devices with limited computational resources. We also report the accuracy (%) of very small VLMs such as SmoIVLM (256M and 500M), medium-sized models like SmoIVLM (2.2B), and large-scale models such as Idefics (80B) across nine multimodal benchmarks. As shown in Figure 18, SmoIVLM with 2.2B parameters consistently achieves the highest accuracy across eight benchmarks, followed by the 500M and then the 256M models. Interestingly, Idefics with 80B parameters yields the lowest performance across most benchmarks. In terms of throughput, the 256M model delivers the highest, followed by the 500M, 2.2B, and finally the 80B model. **A higher throughput indicates better efficiency.** These results highlight a critical insight: achieving optimal performance on edge or pervasive IoT devices requires a careful balance between accuracy and efficiency, tailored to the specific constraints of the deployment hardware, such as memory and GPU availability.

8 | APPLICATIONS

VLMs have demonstrated exceptional performance in tasks such as image captioning, VQA, and document understanding. The development of compact models has extended their applicability to real-time applications, allowing for deployment on resource-constrained devices. These models are utilized across various domains, including robotics, medical applications, autonomous driving, augmented and virtual reality (AR/VR), and smart surveillance. Table 5 provides datasets to train VLMs for various downstream applications.

8.1 | Autonomous Driving

VLMs play a crucial role in autonomous driving by enabling robust scene understanding, decision-making, and natural language-based interactions. DriveVLM Tian et al. (2024) enhances autonomous driving by leveraging VLMs for advanced scene understanding and planning. It leverages the chain-of-thought (CoT) process with modules for scene description, analysis, and hierarchical planning. To address spatial reasoning and computing limits, DriveVLM-Dual combines VLM-based reasoning with traditional 3D perception and planning, resulting in improved real-time decision-

making. DriveVLM demonstrates its effectiveness through successful deployment in real-world scenarios. To address the lack of natural language integration for interpretable decision-making in autonomous driving, Park et al. (2024) introduce an instruction tuning dataset and train a multimodal model called VLAAD for enhanced scene understanding and reasoning. V2X-VLM You et al. (2024) performs end-to-end vehicle-infrastructure cooperative autonomous driving for enhanced situational awareness and optimized trajectory planning.

8.2 | Medical Applications

VLMs are used extensively in medical applications for question-answering and medical report generation. They also help interpret medical images by combining visual and textual information for better diagnosis. MedViLL Moon et al. (2022) performs vision-language pre-training and multi-modal representation learning for medical applications. It improves diagnostic classification, medical image report retrieval, visual question answering, and radiology report generation with a BERT-based architecture Devlin et al. (2019) and a novel attention masking method. PubMedCLIP Eslami et al. (2023) fine-tunes CLIP for medical visual question answering (MedVQA) using medical image-text pairs from PubMed. Unlike previous approaches, it is not limited to certain body regions and supports several imaging modalities (X-ray, CT, MRI). SERPENT-VLM Kapadnis et al. (2024) reduces hallucinations and improves radiology report generation by refining image-text alignment using a self-supervised loss. It outperforms LLaVA-Med and BiomedGPT on IU X-ray and ROCO datasets while maintaining robustness against noisy images. Med-MoE Jiang et al. (2024) enables lightweight medical VLMs using Mixture-of-Experts, optimizing efficiency for Med-VQA and classification tasks while reducing compute needs.

8.3 | Robotic Navigation and Manipulation

Recently, considerable efforts have been directed toward integrating VLMs for robotic navigation and manipulation, which are crucial for search and rescue (SaR) operations. Effective robotic navigation and manipulation in challenging environments require a precise understanding of physical properties and geometric relationships. Geometric awareness includes assessing whether an object can fit inside another or identifying appropriate cover, enabling robots to make informed decisions and interact safely with their surroundings. Physical grounding is essential for search and rescue operations and hazard detection. Gao et al. (2024c) introduce *PHYSOBJECTS*, a dataset incorporating physical concepts like mass, fragility, deformability, and density. They fine-tune a VLM on this dataset and propose a robotic manipulation framework where the LLM queries the VLM, receives responses, and formulates an execution plan. VLM-GroNav Elnoor et al. (2024) integrates a VLM-based reasoning module with physical grounding to evaluate terrain properties like slipperiness and deformability. The framework is tested on two robots: Ghost Vision 60¹¹ and Clearpath Husky¹². Ahmad et al. (2024) integrate VLMs with Behavior Trees (BTs) to detect, identify, and recover from failures in robotic tasks. The VLM analyzes visual input to recognize failures, suggest missing conditions and update the BT to handle similar failures in the future. VLM-Social-Nav Song et al. (2025) leverages VLMs to interpret social context and compute a navigation cost, enabling robots to make socially aware decisions in human environments.

8.4 | Smart Surveillance

VLMs have transformed smart surveillance by enabling advanced scene understanding and contextual reasoning. Li et al. (2024d) introduce a FL framework for domain-specific VLMs, enabling collaborative fine-tuning of large multimodal models for smart city safety and urban operation management. Silva et al. (2025) introduces a novel VLM-based pipeline

¹¹<https://www.ghostrobotics.io/vision-60>

¹²<https://clearpathrobotics.com/husky-a300-umanned-ground-vehicle-robot/>

TABLE 5 Datasets with image-text pairs for training VLMs in various applications. Refer to Zhou et al. (2023); Hartsock and Rasool (2024) for more datasets on autonomous driving and medical applications, respectively.

Dataset	Year	Key Features	Link
AUTONOMOUS DRIVING DATASETS			
BDD-X Kim et al. (2018)	2018	Dataset contains over 26K activities in over 8.4M frames. Train and test set contain 5,597 and 656 videos respectively. Used for action explanation.	
TOUCHDOWN Chen et al. (2019)	2019	Used for natural language navigation and spatial reasoning in urban environments. 6,526 training, 1,391 development, 1,409 test for navigation; 17,880 training, 3,836 development, 3,859 test for SDR.	
HAD Kim et al. (2019)	2019	Contains 30 hours of driving data with natural language advice. Primarily used for Human-to-Vehicle Advice.	
Talk2Car Deruyttere et al. (2019)	2020	Provides free-form natural language commands for autonomous driving. Built on nuScenes, with multimodal sensor data (RGB, LIDAR, RADAR, GPS, semantic maps, 3D bounding boxes). It has 8349 train samples and 2447 test samples.	
CARLA-NAV Jain et al. (2022)	2022	It has video sequences from 8 maps and 14 weather conditions. It contains dynamic scenes and trajectory annotations for real-time navigation.	
Talk2BEV Dewangan et al. (2023)	2023	1000 human-annotated BEV scenarios with 20,000+ questions and ground-truth answers from the nuScenes dataset. Used for open-loop decision-making.	
DRAMA Malla et al. (2023)	2023	17,785 urban traffic clips from Tokyo with synchronized video, CAN signals, and IMU data, featuring annotations like Q/A, bounding boxes, and driver suggestions.	
MEDICAL DATASETS			
ROCO Friedrich et al. (2017)	2018	A large-scale medical imaging dataset featuring radiology and non-radiology images with captions, keywords, UMLS Semantic Types, and Concept Unique Identifiers (CUIs), useful for image captioning, classification, and retrieval.	
MIMIC-CXR Johnson et al. (2024b)	2019	377,110 chest X-ray images in DICOM format with corresponding free-text radiology reports. It includes patient and study identifiers, structured metadata, and de-identified annotations for research in medical imaging.	
MIMIC-CXR-JPG Johnson et al. (2024a, 2019)	2019	MIMIC-CXR-JPG uses JPG format with structured labels, while MIMIC-CXR provides DICOM images with free-text reports.	
MediCaT Subramanian et al. (2020)	2020	Contains 217,060 medical figures with captions, subfigure annotations, and inline references from PubMed Central and S2ORC.	
PMC-OA Lin et al. (2023)	2023	Biomedical dataset with 1.65M image-caption pairs. Commonly used for retrieval, classification, and VQA tasks.	
ROBOT NAVIGATION & MANIPULATION DATASETS			
CC3M Sharma et al. (2018)	2018	Contains 3 million image-text pairs collected from the web. Helps robots understand visual scenes through language grounding.	Webpage
MQA Deng et al. (2021)	2021	Simulation-based dataset for manipulation question answering (MQA). It includes scene variations, Q&A pairs, and real-world transferability.	
ManipVQA Huang et al. (2024a)	2024	It introduces a VQA format for robotic affordance understanding by integrating tool detection, affordance recognition, and physical concept grounding.	
PHYSOBJECTS Gao et al. (2024b)	2024	Object-centric dataset with 39.6K crowd-sourced and 417K automated physical concept annotations for household objects. Used for robotic manipulation & planning.	Webpage
SMART SURVEILLANCE DATASETS			
COYO-700M Byeon et al. (2022)	2022	747M image-text pairs useful for scene understanding and anomaly detection	
FaceCaption-15M Dai et al. (2024)	2024	Useful for smart surveillance and security as it provides detailed facial image-text pairs, enabling advanced facial recognition, identity verification and suspect tracking.	

for efficient video analysis. They reduce storage space by replacing video data with detailed textual summaries from CCTV feeds. Video-ChatGPT [Maaz et al. \(2024\)](#) provides detailed video understanding and conversational AI capabilities, which can be integrated for smart surveillance by fine-tuning it on security footage for real-time anomaly detection and event summarization.

8.5 | Augmented Reality (AR)

VLMs have emerged as an effective tool for enhancing augmented reality experiences. ViDDAR [Xiu et al. \(2025\)](#) detects obstruction and information manipulation attacks for enhancing safety and usability in AR. It uses VLMs to analyze virtual content interactions and assess their impact on real-world scene understanding. ViDDAR employs a user-edge-cloud architecture to balance detection accuracy and latency. [Duan et al. \(2025\)](#) introduce DiverseAR, the first dataset designed to evaluate the capability of VLMs to identify and describe virtual content at varying levels of AR scene complexity. TAGGAR [Stover and Bowman \(2024\)](#) is a general-purpose AR task guidance system that uses VLMs to generate automated visual instructions from natural language and images. It eliminates the need for expert-placed AR visuals or CAD models by allowing operators to specify tasks with text and images.

9 | OPEN CHALLENGES AND FUTURE DIRECTIONS

Despite the proliferation of Vision-Language Models (VLMs) in recent months, their deployment on resource-constrained devices for real-time applications remains a substantial challenge. A primary limitation arises from the computational complexity and large feature representations required to effectively align visual and textual modalities. These high-dimensional embeddings demand significant memory and processing resources, which are often unavailable on edge devices. We outline the key challenges in adapting VLMs for such environments.

9.1 | Accuracy Vs Efficiency Tradeoff

While foundational VLMs can provide great accuracy for various tasks, they are inefficient in terms of memory and computational requirements. Techniques such as quantization and pruning were developed to fit the VLMs on the edge [Yang et al.](#) Matryoshka Quantization (MatQuant) [Nair et al. \(2025\)](#) improves efficiency by enabling a single model to operate at multiple precision levels, achieving up to 10% higher accuracy for int2 models than standard Quantization-Aware Training.

Benchmarking results have shown that large-scale Vision-Language Models (VLMs) achieve high accuracy across a wide range of tasks and domains [Yue et al. \(2024b\)](#). Although researchers are also developing small VLM models (sub-billion and <3B parameters) for multimodal multidomain tasks [Marafioti et al. \(a\)](#) [Zhou et al. \(2024\)](#) [Marafioti et al. \(b\)](#), the architecture and training data plays an important role in using benchmarking dataset to test the efficacy of the model. However, this raises a critical question: *Must edge-deployed VLMs achieve state-of-the-art performance across all tasks?* In practice, VLMs on edge devices are often designed to perform narrow, task-specific functions with high efficiency and accuracy. The real challenge lies in developing specialized VLMs tailored for specific edge applications, which often require compact architectures and context-aware capabilities.

While techniques such as knowledge distillation, low-rank adaptation (LoRA), and adapter-based tuning offer promising solutions for compressing and specializing large models, they remain limited in their ability to capture the full complexity and adaptability needed for task-specific reasoning on resource-constrained hardware [Wang et al. \(2025a\)](#). Bridging this gap calls for continued advances in task-aware model compression, self-supervised learning at the edge, and incremental adaptation mechanisms capable of responding to environmental feedback in real time.

9.2 | Agentic AI and Distributed VLMs @Edge

As artificial intelligence systems become increasingly embedded in dynamic, real-world environments, the need for agents capable of perceiving, reasoning, and acting autonomously has intensified [Acharya et al. \(2025\)](#). However, deploying these capabilities in the real world, especially in settings like robotics, autonomous vehicles, and smart infrastructure, requires moving beyond centralized, cloud-based inference. This leads to the emerging paradigm of distributed VLMs at the edge, where multiple lightweight or specialized models collaborate across heterogeneous devices and contexts [Tallam \(2025\)](#). Multi-agent systems may use shared or federated VLMs to jointly interpret scenes, coordinate tasks, and share knowledge representations [Yang and Dong \(2025\)](#). This gives rise to a requirement for a modular architecture where agents may consist of distributed components (e.g., local perception + cloud-based planning), or fully edge-deployed systems with swappable VLM modules based on task requirements. Distributed agents must coordinate semantic knowledge across bandwidth-limited links while maintaining consistent interpretations of multimodal inputs [Zhu et al. \(2025\)](#). Agents must adapt their VLMs to new tasks, domains, and environmental changes without catastrophic forgetting or overfitting. This also calls for Vision encoders and task-specific decoders to share generic features between agents and use task-specific decoders at the receiver to extract meaningful information for different tasks. One such example includes collecting RGB, LiDAR, and IMU information from robots to (a) extract the type of surface using LiDAR and IMU, (b) use RGB and LiDAR for object detection and classification, and (c) use RGB and IMU to detect deformities on the surface.

9.3 | On-the-fly Fine-Tuning of VLMs

On-the-fly fine-tuning methodologies aim to dynamically adapt VLMs to new data or environments without full retraining [Malladi et al. \(2024\)](#). These methods are critical for applications in robotics, autonomous systems, wearable devices, and mobile platforms, where VLMs must evolve with changing tasks and environments [Tang et al. \(2024\)](#). Some of the existing techniques include meta-learning and test-time adaptation. Meta-learning involves training models to quickly adapt to novel tasks using limited examples. In the VLM domain, meta-learning is instrumental in facilitating few-shot learning, cross-domain generalization, and personalized user adaptation, particularly in low-resource scenarios [Najdenkoska et al. \(2023\)](#) [Ma et al. \(2024\)](#) [Hu and Keller \(2023\)](#). Test-time adaptation enables models to self-adjust during inference using only unlabeled test samples [Karmanov et al. \(2024b\)](#) [Farina et al. \(2024b\)](#) [Farina et al. \(2024c\)](#). Unlike meta-learning, TTA does not require episodic task design or access to training data. It is particularly suitable for dynamic, real-time environments where domain shifts or evolving user contexts occur frequently. However, these techniques are still immature to be adapted for edge scenarios. Some of the immediate challenges include: (a) designing lightweight and scalable adaptation frameworks for edge deployment with the above-mentioned techniques; (b) developing unified multimodal task abstractions for few-shot and episodic learning.

9.4 | Multimodal VLM @Edge

While Vision-Language Models (VLMs) are often referred to as multimodal large language models, their modality coverage is typically limited to vision and language, with some models extending to audio or basic spatial context. However, there remains significant untapped potential in broadening the multimodal spectrum to include diverse sensor data, which could substantially enhance model accuracy, contextual understanding, and real-time decision-making across various application domains.

Recent advancements in human activity recognition (HAR) and affective computing suggest that integrating additional sensory modalities can complement visual and linguistic inputs, providing rich, context-aware representations. For instance: Inertial Measurement Units (IMUs) and earable sensors offer continuous, low-latency streams of motion and physiological data that are especially valuable in recognizing fine-grained human activities. Their integration into

VLM frameworks could help models distinguish between visually similar actions that differ in physical dynamics (e.g., jogging vs. limping). Millimeter-Wave Radar (mmWave) sensors have been shown to accurately detect human posture and micro-gestures without relying on cameras. In the mmCLIP framework [Cao et al. \(2024\)](#), radar signals are aligned with vision-language embeddings to improve privacy-preserving human activity recognition, offering robustness in low-light or occluded environments where cameras fail. Electroencephalography (EEG) signals provide a direct interface to brain activity, enabling models to infer cognitive and emotional states in real-time. Recent work [Li et al. \(2024a\)](#) has integrated EEG with VLM for visual captioning. Audio signals remain a powerful yet underutilized modality. Sonic-VisionLM [Xie et al. \(2024b\)](#) showcases how integrating audio with visual data enhances temporal grounding in video understanding. For instance, matching sounds of footsteps, speech, or environmental cues with corresponding visual scenes allows for more accurate event recognition and scene parsing.

These examples demonstrate the value of moving beyond the traditional image-text paradigm toward truly multimodal VLM architectures. Integrating such diverse sensor modalities can enrich semantic representation, improve generalization, and enable robust performance in complex, real-world scenarios—particularly in wearable computing, robotics, autonomous vehicles, and assistive technologies.

9.5 | Reasoning for Cohesive Environment

The integration of Human-in-the-Loop strategies with Vision-Language Models presents promising opportunities for enhancing the performance, adaptability, and trustworthiness of AI systems in real-world applications to build a cohesive environment. However, this integration introduces several research challenges that must be addressed to ensure effective and reliable deployment.

Model Interpretability and Transparency: VLMs typically function as black-box systems, making it difficult to understand the reasoning behind their predictions. This lack of interpretability reduces user trust and limits the value of human feedback. Explainable AI techniques such as visual attention maps [Selvaraju et al. \(2017\)](#), natural language rationales [Camburu et al. \(2018\)](#), and counterfactual reasoning [Goyal et al. \(2019b\)](#) are being explored to bridge this gap. Nonetheless, robust and scalable interpretability methods tailored to multimodal inputs remain an open research problem.

Confidence Calibration and Uncertainty Estimation: Human-in-the-loop systems depend on the model's ability to recognize its own uncertainty and defer to human input when appropriate. Poorly calibrated confidence scores can lead to either over-reliance on the model or unnecessary human intervention. Methods such as temperature scaling [Guo et al. \(2017\)](#), Bayesian neural networks [Kendall and Gal \(2017\)](#), and Monte Carlo Dropout [Gal and Ghahramani \(2016\)](#) have been proposed to improve uncertainty estimation in deep learning, but their application in VLMs, especially under dynamic multimodal conditions, is still evolving.

Bias, Fairness, and Trust in Human Feedback: Incorporating human feedback does not guarantee fairness; in fact, it may introduce or reinforce biases. Research into adversarial human feedback, trust calibration mechanisms [Okamura and Yamada \(2020\)](#), and feedback quality filtering aims to mitigate these risks. Ensuring equitable and ethical behavior in Human-in-the-loop-VLM systems [Duan et al. \(2024\)](#) [McGrath et al. \(2024\)](#) requires robust governance frameworks and transparent user interaction logging.

9.6 | Hallucination

An emerging challenge in optimizing VLMs for edge environments is *hallucination*, where models produce confident but factually incorrect outputs. The hallucinations in VLMs can stem from:

Object Hallucination: The VLM can hallucinate objects not present in the scene. These arise due to contexts in the scene or vague text prompts. For instance, an image with a dining table, plates, and glasses could lead the VLM models

to believe that there is food and drinks on the table. The BLIP model outputs "Dining Table with food and drinks" when there is no food or drink. Another example would be an image with Dogs in a park and a prompt to explain the image, the model generates, "It is a Dog Park," which can be confused with Dogs in a regular Park. The difference is in identifying the leash in regular parks vs unleashed dogs in a Dog park. Such intricate details might have been missed during the training process.

Relation Hallucination: The VLM model could hallucinate relations between objects in a given scene. For instance, a man and a dog in a scene could be hallucinated for "Man playing fetch with Dog".

Temporal Hallucination: The VLM model could hallucinate the actions performed in a scene. For instance, a woman standing on a cliff with a harness could be hallucinated as "Woman bungee jumping from the cliff".

Although not directly evaluated for hallucination, [Yuan et al. \(2022\)](#) show that post-training quantization distorts activation distributions, crucial for semantic alignment. This increases the risk of hallucinated outputs in multimodal tasks. [Lewis et al. \(2025\)](#) show that knowledge distillation (KD) leads to hallucination due to higher exposure bias and overfitting to teacher's labels. [Baqar and Khanda \(2025\)](#) show that LoRA leads to hallucinations due to static pre-trained knowledge. These effects are particularly concerning in safety-critical applications like medical imaging or autonomous driving, where factual grounding is nonnegotiable.

Some studies explore methods to reduce hallucination in vision-language models. SERPENT-VLM [Kapadnis et al. \(2024\)](#) introduces a self-supervised loss between the pooled image representation and the contextual representation of the generated text, which aligns vision and language features to reduce hallucination. This strategy can also be incorporated in compressed settings to maintain semantic and textual consistency. AdaVIB [Bai et al. \(2025\)](#) mitigates hallucinations by using a variational information bottleneck that introduces stochastic noise to improve vision language alignment. Jiang et al. [Jiang et al. \(2025\)](#) suggest editing the model's latent representation to reduce hallucination by 27% for LLaVa models. Some recent methods use decoding techniques [Augustin et al. \(2025\)](#) [Favero et al. \(2024\)](#) [Yang et al. \(2025\)](#) to mitigate the hallucination. As vision-language models are increasingly used in edge and distributed settings, future research should focus on developing compression-aware grounding objectives and uncertainty estimation techniques to mitigate hallucination. Models such as Grounded-SAM [Ren et al. \(2024\)](#) help reduce object hallucinations as they require users to specify objects of interest, which may be more suitable for edge environments and applications that specifically look for known objects in the scene.

9.7 | Security and Privacy

When VLMs are deployed on end devices, they become vulnerable to adversarial attacks such as Jacobian-based Saliency Map Attack (JSMA) [Wiyatno and Xu \(2018\)](#), which can manipulate model predictions through carefully crafted perturbations. To mitigate these threats, adversarial defense techniques, such as adversarial training [Zhang et al. \(2024c\)](#) are employed to enhance model resilience against such attacks. In a federated setting, shared gradients are susceptible to inversion attacks [Zhu et al. \(2019\)](#). These attacks reconstruct private data and compromise privacy. To counteract this, techniques such as differential privacy and gradient pruning [Zhu et al. \(2019\)](#) are used. Differentially Private Federated Prompt Learning (DP-FPL) [Tran et al. \(2025\)](#) balances personalization, generalization, and privacy in federated learning for multimodal LLMs. It uses low-rank factorization with a residual term to preserve expressiveness while applying both global and local differential privacy to mitigate privacy risks without significantly degrading performance. However, an honest-but-curious server may still analyze shared updates to infer patterns. Future research should address these challenges to improve the robustness of VLMs in distributed environments. Secure encryption is crucial for cooperative perception tasks in dynamic autonomous systems to prevent adversarial interceptions. AES-256 enables privacy-preserving data transmission. However, with the increasing use of VLMs in distributed applications such as robotics, lightweight and robust encryption algorithms are required to ensure secure information transfer while minimizing computational overhead.

10 | CONCLUSION

Vision-Language Models (VLMs) have rapidly advanced in recent years, demonstrating impressive capabilities in multi-modal understanding, visual question answering, image captioning, and grounded reasoning. In this survey, we present a comprehensive and structured review of efficient vision-language models (VLMs). We begin by motivating the need for optimizing VLMs for edge-centric applications and subsequently examine key techniques including pre-deployment strategies, fine-tuning methodologies, and runtime optimizations. The pre-deployment section encompasses quantization, low-rank approximation, pruning, knowledge distillation, and mixture of experts. For efficient fine-tuning, we provide a detailed overview of parameter-efficient and memory-efficient approaches. The runtime optimization section discusses token reduction techniques and test-time adaptation mechanisms. We also detail privacy-preserving distributed VLM approaches, such as federated learning and split learning. Finally, we highlight various lightweight VLMs, discuss their applications, and offer insights into the accuracy-efficiency trade-off of VLMs.

In conclusion, we outline several open challenges in the development and deployment of Vision-Language Models (VLMs) and highlight key questions that remain unanswered within the research community. A fundamental consideration is whether edge-deployed VLMs should be designed for multitasking or optimized for task-specific performance. Depending on the application domain and system constraints, there is a compelling argument for tailoring VLMs to maximize efficiency and accuracy for narrowly defined tasks. Such task-oriented VLMs would benefit from the ability to adapt on-the-fly to dynamic environments, enabling real-time contextual learning and robustness to unforeseen inputs. However, the practical implementation of on-the-fly adaptation techniques remains largely unproven in real-world settings, with few reproducible, evidence-based studies demonstrating their effectiveness at the edge.

Moreover, as VLMs are increasingly adopted in safety-critical and human-centered systems, there are growing concerns regarding their robustness, fairness, and trustworthiness. These models can generate plausible yet incorrect outputs, propagate harmful social biases, or become vulnerable to adversarial inputs, undermining their reliability. Addressing these issues necessitates improved model interpretability, calibrated confidence estimation, and the integration of human-in-the-loop mechanisms to ensure meaningful oversight and corrective intervention. As the field continues to evolve, answering these foundational questions and overcoming the aforementioned limitations will be essential to realizing reliable, adaptive, and ethically aligned multimodal AI systems for deployment in real-world edge and distributed environments.

11 | CONFLICT OF INTEREST

The authors have declared no conflicts of interest for this article.

references

- Acharya, D. B., Kuppan, K. and Divya, B. (2025) Agentic ai: Autonomous intelligence for complex goals—a comprehensive survey. *IEEE Access*, **13**, 18912–18936.
- Agarwalla, M., Kumar, H., Dandekar, R., Dandekar, R. and Panat, S. (2025) Nanovlms: How small can we go and still make coherent vision language models? URL: <https://arxiv.org/abs/2502.07838>.
- Agiza, A., Neseem, M. and Reda, S. (2024) Mtlora: Low-rank adaptation approach for efficient multi-task learning. In *Proceedings of the IEEE/CVF Conference on Computer Vision and Pattern Recognition (CVPR)*, 16196–16205.
- Ahmad, F., Styrod, J. and Krueger, V. (2024) Addressing failures in robotics using vision-based language models (vlms) and behavior trees (bt). URL: <https://arxiv.org/abs/2411.01568>.
- AI, M. () Moondream: The open source vlm that runs everywhere. <https://moondream.ai/>. Accessed: February 2025.
- Ardakani, A., Haan, A., Tan, S., Popovici, D. T., Cheung, A., Iancu, C. and Sen, K. (2024) SlimFit: Memory-efficient fine-tuning of transformer-based models using training dynamics. In *Proceedings of the 2024 Conference of the North American Chapter of the Association for Computational Linguistics: Human Language Technologies (Volume 1: Long Papers)* (eds.

- K. Duh, H. Gomez and S. Bethard), 6218–6236. Mexico City, Mexico: Association for Computational Linguistics. URL: <https://aclanthology.org/2024.naacl-long.345/>.
- Augustin, M., Neuhaus, Y. and Hein, M. (2025) Dash: Detection and assessment of systematic hallucinations of vlms. URL: <https://arxiv.org/abs/2503.23573>.
- Bai, J., Guo, H., Peng, Z., Yang, J., Li, Z., Li, M. and Tian, Z. (2025) Mitigating hallucinations in large vision-language models by adaptively constraining information flow. URL: <https://arxiv.org/abs/2502.20750>.
- Bai, Y., Zhao, H., Lin, Z., Kale, A., Gu, J., Yu, T., Kim, S. and Fu, Y. (2024) Advancing vision-language models with adapter ensemble strategies. In *Findings of the Association for Computational Linguistics: EMNLP 2024* (eds. Y. Al-Onaizan, M. Bansal and Y.-N. Chen), 15702–15720. Miami, Florida, USA: Association for Computational Linguistics. URL: <https://aclanthology.org/2024.findings-emnlp.921/>.
- Bao, H., Dong, L. and Wei, F. (2021) Beit: Bert pre-training of image transformers. *ArXiv*, abs/2106.08254. URL: <https://api.semanticscholar.org/CorpusID:235436185>.
- Baqar, M. and Khanda, R. (2025) Hallucinations and truth: A comprehensive accuracy evaluation of rag, lora and dora. URL: <https://arxiv.org/abs/2502.10497>.
- Bondarenko, Y., Chiaro, R. D. and Nagel, M. (2024) Low-rank quantization-aware training for llms. URL: <https://arxiv.org/abs/2406.06385>.
- Byeon, M., Park, B., Kim, H., Lee, S., Baek, W. and Kim, S. (2022) Coyo-700m: Image-text pair dataset. <https://github.com/kakaobrain/coyo-dataset>.
- Cai, K., Duan, Z., Liu, G., Fleming, C. and Lu, C. X. (2024) Self-adapting large visual-language models to edge devices across visual modalities. URL: <https://arxiv.org/abs/2403.04908>.
- Camburu, O.-M., Rocktäschel, T., Lukasiwicz, T. and Blunsom, P. (2018) e-snli: Natural language inference with natural language explanations. In *Advances in Neural Information Processing Systems (NeurIPS)*.
- Cao, Q., Paranjape, B. and Hajishirzi, H. (2023) Pumer: Pruning and merging tokens for efficient vision language models. *ArXiv*, abs/2305.17530. URL: <https://api.semanticscholar.org/CorpusID:258959382>.
- Cao, Q., Xue, H., Liu, T., Wang, X., Wang, H., Zhang, X. and Su, L. (2024) mmclip: Boosting mmwave-based zero-shot har via signal-text alignment. In *Proceedings of the 22nd ACM Conference on Embedded Networked Sensor Systems, SenSys '24*, 184–197. New York, NY, USA: Association for Computing Machinery. URL: <https://doi.org/10.1145/3666025.3699331>.
- Chen, H., Suhr, A., Misra, D., Snively, N. and Artzi, Y. (2019) Touchdown: Natural language navigation and spatial reasoning in visual street environments. In *2019 IEEE/CVF Conference on Computer Vision and Pattern Recognition (CVPR)*, 12530–12539.
- Chen, L., Li, J., Dong, X., Zhang, P., Zang, Y., Chen, Z., Duan, H., Wang, J., Qiao, Y., Lin, D. et al. (2024a) Are we on the right way for evaluating large vision-language models? *arXiv preprint arXiv:2403.20330*.
- Chen, M., Shao, W., Xu, P., Wang, J., Gao, P., Zhang, K., Qiao, Y. and Luo, P. (2024b) Efficientqat: Efficient quantization-aware training for large language models.
- Cheng, C., Song, L., Xue, R., Wang, H., Sun, H., Ge, Y. and Shan, Y. (2023) Meta-adapter: an online few-shot learner for vision-language model. In *Proceedings of the 37th International Conference on Neural Information Processing Systems, NIPS '23*. Red Hook, NY, USA: Curran Associates Inc.
- Cho, E., Kim, J. and Kim, H. J. (2023) Distribution-aware prompt tuning for vision-language models. In *2023 IEEE/CVF International Conference on Computer Vision (ICCV)*, 21947–21956.
- Chu, X., Qiao, L., Lin, X., Xu, S., Yang, Y., Hu, Y., Wei, F., Zhang, X., Zhang, B., Wei, X. and Shen, C. (2023) Mobilevlm: A fast, strong and open vision language assistant for mobile devices. *ArXiv*, abs/2312.16886. URL: <https://api.semanticscholar.org/CorpusID:266573855>.
- Dai, D., Li, Y., Liu, Y., Jia, M., Yuanhui, Z. and Wang, G. (2024) 15m multimodal facial image-text dataset. URL: <https://arxiv.org/abs/2407.08515>.
- Dao, T. (2024) FlashAttention-2: Faster attention with better parallelism and work partitioning. In *International Conference on Learning Representations (ICLR)*.
- DeepSeek-AI, Guo, D., Yang, D., Zhang, H., Song, J., Zhang, R., Xu, R., Zhu, Q., Ma, S., Wang, P., Bi, X., Zhang, X., Yu, X., Wu, Y., Wu, Z. F., Gou, Z., Shao, Z., Li, Z., Gao, Z., Liu, A., Xue, B., Wang, B., Wu, B., Feng, B., Lu, C., Zhao, C., Deng, C., Zhang, C., Ruan, C., Dai, D., Chen, D., Ji, D., Li, E., Lin, F., Dai, F., Luo, F., Hao, G., Chen, G., Li, G., Zhang, H., Bao, H., Xu, H., Wang, H., Ding, H., Xin, H., Gao, H., Qu, H., Li, H., Guo, J., Li, J., Wang, J., Chen, J., Yuan, J., Qiu, J., Li, J., Cai, J. L., Ni, J., Liang, J., Chen, J., Dong, K., Hu, K., Gao, K., Guan, K., Huang, K., Yu, K., Wang, L., Zhang, L., Zhao, L., Wang, L., Zhang, L., Xu, L., Xia, L., Zhang, M., Zhang, M., Tang, M., Li, M., Wang, M., Li, M., Tian, N., Huang, P., Zhang, P., Wang, Q., Chen, Q., Du, Q., Ge, R., Zhang, R., Pan, R., Wang, R., Chen, R. J., Jin, R. L., Chen, R., Lu, S., Zhou, S., Chen, S., Ye, S., Wang, S., Yu, S., Zhou, S., Pan, S., Li, S. S., Zhou, S., Wu, S., Ye, S., Yun, T., Pei, T., Sun, T., Wang, T., Zeng, W., Zhao, W., Liu, W., Liang, W., Gao, W., Yu, W., Zhang, W., Xiao, W. L., An, W., Liu, X., Wang, X., Chen, X., Nie, X., Cheng, X., Liu, X., Xie, X., Liu, X., Yang, X., Li, X., Su, X., Lin, X., Li, X. Q., Jin, X., Shen, X., Chen, X., Sun, X., Wang, X., Song, X., Zhou, X., Wang, X., Shan, X., Li, Y. K., Wang, Y. Q., Wei, Y. X., Zhang, Y., Xu, Y., Li, Y., Zhao, Y., Sun, Y., Wang, Y., Yu, Y., Zhang, Y., Shi, Y., Xiong, Y., He, Y., Piao, Y., Wang, Y., Tan, Y., Ma, Y., Liu, Y., Guo, Y.,

- Ou, Y., Wang, Y., Gong, Y., Zou, Y., He, Y., Xiong, Y., Luo, Y., You, Y., Liu, Y., Zhou, Y., Zhu, Y. X., Xu, Y., Huang, Y., Li, Y., Zheng, Y., Zhu, Y., Ma, Y., Tang, Y., Zha, Y., Yan, Y., Ren, Z. Z., Ren, Z., Sha, Z., Fu, Z., Xu, Z., Xie, Z., Zhang, Z., Hao, Z., Ma, Z., Yan, Z., Wu, Z., Gu, Z., Zhu, Z., Liu, Z., Li, Z., Xie, Z., Song, Z., Pan, Z., Huang, Z., Xu, Z., Zhang, Z. and Zhang, Z. (2025) Deepseek-r1: Incentivizing reasoning capability in llms via reinforcement learning. URL: <https://arxiv.org/abs/2501.12948>.
- Deng, J., Dong, W., Socher, R., Li, L.-J., Li, K. and Fei-Fei, L. (2009) Imagenet: A large-scale hierarchical image database. In *2009 IEEE Conference on Computer Vision and Pattern Recognition*, 248–255.
- Deng, Y., Guo, D., Guo, X., Zhang, N., Liu, H. and Sun, F. (2021) Mqa: Answering the question via robotic manipulation. In *Proceedings of Robotics: Science and Systems*.
- Deruyttere, T., Vandenhende, S., Grujicic, D., Van Gool, L. and Moens, M. F. (2019) Talk2car: Taking control of your self-driving car. In *Proceedings of the 2019 Conference on Empirical Methods in Natural Language Processing and the 9th International Joint Conference on Natural Language Processing (EMNLP-IJCNLP)*, 2088–2098.
- Devlin, J., Chang, M.-W., Lee, K. and Toutanova, K. (2019) BERT: Pre-training of deep bidirectional transformers for language understanding. In *Proceedings of the 2019 Conference of the North American Chapter of the Association for Computational Linguistics: Human Language Technologies, Volume 1 (Long and Short Papers)* (eds. J. Burstein, C. Doran and T. Solorio), 4171–4186. Minneapolis, Minnesota: Association for Computational Linguistics. URL: <https://aclanthology.org/N19-1423/>.
- Dewangan, V., Choudhary, T., Chandhok, S., Priyadarshan, S., Jain, A., Singh, A., Srivastava, S., Jatavallabhula, K. and Krishna, M. (2023) Talk2bev: Language-enhanced bird's-eye view maps for autonomous driving. In *arXiv*.
- Dong, P., Lu, L., Wu, C., Lyu, C., Yuan, G., Tang, H. and Wang, Y. (2023) Packqvit: faster sub-8-bit vision transformers via full and packed quantization on the mobile. In *Proceedings of the 37th International Conference on Neural Information Processing Systems*, NIPS '23. Red Hook, NY, USA: Curran Associates Inc.
- Du, Y., Liu, Z., Li, J. and Zhao, W. X. (2022) A survey of vision-language pre-trained models. In *International Joint Conference on Artificial Intelligence*. URL: <https://api.semanticscholar.org/CorpusID:247026006>.
- Duan, L., Xiu, Y. and Gorlatova, M. (2025) Advancing the understanding and evaluation of ai-generated scenes: When vision-language models shine and stumble. URL: <https://arxiv.org/abs/2501.13964>.
- Duan, W., Zhou, S., Scalia, M. J., Yin, X., Weng, N., Zhang, R., Freeman, G., McNeese, N., Gorman, J. and Tolston, M. (2024) Understanding the involvement of trust over time within human-ai teams. *Proc. ACM Hum.-Comput. Interact.*, **8**. URL: <https://doi.org/10.1145/3687060>.
- Elnoor, M., Weerakoon, K., Seneviratne, G., Xian, R., Guan, T., Jaffar, M. K. M., Rajagopal, V. and Manocha, D. (2024) Robot navigation using physically grounded vision-language models in outdoor environments. URL: <https://arxiv.org/abs/2409.20445>.
- Eslami, S., Meinel, C. and de Melo, G. (2023) PubMedCLIP: How much does CLIP benefit visual question answering in the medical domain? In *Findings of the Association for Computational Linguistics: EAACL 2023* (eds. A. Vlachos and I. Augenstein), 1181–1193. Dubrovnik, Croatia: Association for Computational Linguistics. URL: <https://aclanthology.org/2023.findings-eacl.88/>.
- Fang, G., Ma, X. T., Mi, M. B. and Wang, X. (2024) Isomorphic pruning for vision models. *arXiv preprint arXiv:2407.04616*.
- Fang, Z., Wang, J., Hu, X., Wang, L., Yang, Y. and Liu, Z. (2021) Compressing visual-linguistic model via knowledge distillation. In *Proceedings of the IEEE/CVF International Conference on Computer Vision (ICCV)*, 1428–1438.
- Farina, M., Franchi, G., Iacca, G., Mancini, M. and Ricci, E. (2024a) Frustratingly easy test-time adaptation of vision-language models. In *Advances in Neural Information Processing Systems* (eds. A. Globerson, L. Mackey, D. Belgrave, A. Fan, U. Paquet, J. Tomczak and C. Zhang), vol. 37, 129062–129093. Curran Associates, Inc. URL: https://proceedings.neurips.cc/paper_files/paper/2024/file/e92cb6f981a2cacb2a710ecaa0d7b141-Paper-Conference.pdf.
- (2024b) Frustratingly easy test-time adaptation of vision-language models. URL: <https://arxiv.org/abs/2405.18330>.
- (2024c) Frustratingly easy test-time adaptation of vision-language models. In *Advances in Neural Information Processing Systems* (eds. A. Globerson, L. Mackey, D. Belgrave, A. Fan, U. Paquet, J. Tomczak and C. Zhang), vol. 37, 129062–129093. Curran Associates, Inc. URL: https://proceedings.neurips.cc/paper_files/paper/2024/file/e92cb6f981a2cacb2a710ecaa0d7b141-Paper-Conference.pdf.
- Farina, M., Mancini, M., Cunegatti, E., Liu, G., Iacca, G. and Ricci, E. (2024d) Multiflow: Shifting towards task-agnostic vision-language pruning. In *Proceedings of the IEEE/CVF Conference on Computer Vision and Pattern Recognition*.
- Favero, A., Zancato, L., Trager, M., Choudhary, S., Perera, P., Achille, A., Swaminathan, A. and Soatto, S. (2024) Multi-modal hallucination control by visual information grounding. URL: <https://arxiv.org/abs/2403.14003>.
- Fawakherji, M., Vazquez, E., Giampa, P. and Bhattarai, B. (2024) Textaug: Test time text augmentation for multimodal person re-identification. In *Proceedings of the IEEE/CVF Winter Conference on Applications of Computer Vision (WACV) Workshops*, 320–329.
- Friedrich, C. M., Pelka, O., Rückert, J., Nensa, F. and Koitka, S. (2017) Radiology objects in context (roco): A multimodal image dataset.
- Fuchs, C., Zanella, M. and Vleeschouwer, C. D. (2025) Online gaussian test-time adaptation of vision-language models. URL:

<https://arxiv.org/abs/2501.04352>.

- Gal, Y. and Ghahramani, Z. (2016) Dropout as a bayesian approximation: Representing model uncertainty in deep learning. In *International Conference on Machine Learning (ICML)*.
- Gao, F., Zhao, Y., Qiu, C. and Wang, X. (2024a) Efficient adapting for vision-language foundation model in edge computing based on personalized and multi-granularity federated learning. In *IEEE INFOCOM 2024 - IEEE Conference on Computer Communications Workshops (INFOCOM WKSHPS)*, 1–6.
- Gao, J., Sarkar, B., Xia, F., Xiao, T., Wu, J., Ichter, B., Majumdar, A. and Sadigh, D. (2024b) Physically grounded vision-language models for robotic manipulation. In *2024 IEEE International Conference on Robotics and Automation (ICRA)*, 12462–12469.
- (2024c) Physically grounded vision-language models for robotic manipulation. In *2024 IEEE International Conference on Robotics and Automation (ICRA)*, 12462–12469.
- Ghosh, A., Acharya, A., Saha, S., Jain, V. and Chadha, A. (2024) Exploring the frontier of vision-language models: A survey of current methodologies and future directions. URL: <https://arxiv.org/abs/2404.07214>.
- Gopalkrishnan, A., Greer, R. and Trivedi, M. (2024) Multi-frame, lightweight & efficient vision-language models for question answering in autonomous driving. URL: <https://arxiv.org/abs/2403.19838>.
- Goyal, Y., Khot, T., Agrawal, A., Summers-Stay, D., Batra, D. and Parikh, D. (2019a) Making the v in vqa matter: Elevating the role of image understanding in visual question answering. *Int. J. Comput. Vision*, **127**, 398–414. URL: <https://doi.org/10.1007/s11263-018-1116-0>.
- Goyal, Y., Wu, Z., Ernst, J., Batra, D., Parikh, D. and Lee, S. (2019b) Counterfactual visual explanations. In *International Conference on Machine Learning (ICML)*.
- Guo, C., Pleiss, G., Sun, Y. and Weinberger, K. Q. (2017) On calibration of modern neural networks. In *International Conference on Machine Learning (ICML)*.
- Guo, T., Guo, S. and Wang, J. (2023) pFedPrompt: Learning personalized prompt for vision-language models in federated learning. In *Proceedings of the ACM Web Conference 2023, WWW '23*, 1364–1374. New York, NY, USA: Association for Computing Machinery. URL: <https://doi.org/10.1145/3543507.3583518>.
- Guo, Y., Fu, Y. and Huang, H. (2019) Real-world image denoising via weighted low rank approximation. In *2019 IEEE International Conference on Multimedia & Expo Workshops (ICMEW)*, 252–257.
- Guo, Y., Wang, G. and Kankanhalli, M. (2024) Pela: Learning parameter-efficient models with low-rank approximation. In *CVPR*.
- Hartsock, I. and Rasool, G. (2024) Vision-language models for medical report generation and visual question answering: a review. *Frontiers in Artificial Intelligence*, **7**. URL: <http://dx.doi.org/10.3389/frai.2024.1430984>.
- He, S., Li, A. and Chen, T. (2024) Rethinking pruning for vision-language models: Strategies for effective sparsity and performance restoration. URL: <https://arxiv.org/abs/2404.02424>.
- Houlsby, N., Giurgiu, A., Jastrzebski, S., Morrone, B., de Laroussilhe, Q., Gesmundo, A., Attariyan, M. and Gelly, S. (2019) Parameter-efficient transfer learning for nlp. *ArXiv*, abs/1902.00751. URL: <https://api.semanticscholar.org/CorpusID:59599816>.
- Hu, H. and Keller, F. (2023) Meta-learning for vision-and-language cross-lingual transfer. URL: <https://arxiv.org/abs/2305.14843>.
- Huang, S., Ponomarenko, I., Jiang, Z., Li, X., Hu, X., Gao, P., Li, H. and Dong, H. (2024a) ManipVQA: Injecting robotic affordance and physically grounded information into multi-modal large language models. URL: <https://arxiv.org/abs/2403.11289>.
- Huang, W., Liu, Y., Qin, H., Li, Y., Zhang, S., Liu, X., Magno, M. and Qi, X. (2025) Billm: pushing the limit of post-training quantization for llms. In *Proceedings of the 41st International Conference on Machine Learning, ICML'24*. JMLR.org.
- Huang, X., Shen, Z., Dong, P. and Cheng, K.-T. (2024b) Quantization variation: A new perspective on training transformers with low-bit precision. *Transactions on Machine Learning Research*. URL: <https://openreview.net/forum?id=MHfoA0Qf6g>.
- Jain, K., Chhangani, V., Tiwari, A., Krishna, K. M. and Gandhi, V. (2022) Ground then navigate: Language-guided navigation in dynamic scenes. *arXiv preprint arXiv:2209.11972*.
- Ji, Y., Liu, Y., Zhang, Z., Zhang, Z., Zhao, Y., Hao, X., Zhou, G., Zhang, X. and Zheng, X. (2025) Enhancing adversarial robustness of vision-language models through low-rank adaptation. URL: <https://arxiv.org/abs/2404.13425>.
- Jiang, N., Kachinthaya, A., Petryk, S. and Gandelsman, Y. (2025) Interpreting and editing vision-language representations to mitigate hallucinations. In *The Thirteenth International Conference on Learning Representations*. URL: <https://openreview.net/forum?id=94kQgWxojH>.
- Jiang, S., Zheng, T., Zhang, Y., Jin, Y., Yuan, L. and Liu, Z. (2024) Med-MoE: Mixture of domain-specific experts for lightweight medical vision-language models. In *Findings of the Association for Computational Linguistics: EMNLP 2024* (eds. Y. Al-Onaizan, M. Bansal and Y.-N. Chen), 3843–3860. Miami, Florida, USA: Association for Computational Linguistics. URL: <https://aclanthology.org/2024.findings-emnlp.221/>.
- Jin, Y., Li, J., Liu, Y., Gu, T., Wu, K., Jiang, Z., He, M., Zhao, B., Tan, X., Gan, Z., Wang, Y., Wang, C. and Ma, L. (2024) Efficient multimodal large language models: A survey. *ArXiv*, abs/2405.10739. URL: <https://api.semanticscholar.org/CorpusID:269899856>.

- Johnson, A., Lungren, M., Peng, Y., Lu, Z., Mark, R., Berkowitz, S. and Horng, S. (2024a) MIMIC-CXR-JPG - Chest Radiographs with Structured Labels (version 2.1.0). URL: <https://doi.org/10.13026/jsn5-t979>.
- Johnson, A., Pollard, T., Mark, R., Berkowitz, S. and Horng, S. (2024b) MIMIC-CXR Database (version 2.1.0). URL: <https://doi.org/10.13026/4jqj-jw95>.
- Johnson, A. E. W., Pollard, T. J., Greenbaum, N. R., Lungren, M. P., ying Deng, C., Peng, Y., Lu, Z., Mark, R. G., Berkowitz, S. J. and Horng, S. (2019) MIMIC-cxr-jpg, a large publicly available database of labeled chest radiographs. URL: <https://arxiv.org/abs/1901.07042>.
- Ju, C., Wang, H., Cheng, H., Chen, X., Zhai, Z., Huang, W., Lan, J., Xiao, S. and Zheng, B. (2024) Turbo: Informativity-driven acceleration plug-in for vision-language large models. In *Computer Vision - ECCV 2024: 18th European Conference, Milan, Italy, September 29–October 4, 2024, Proceedings, Part XLVI*, 436–455. Berlin, Heidelberg: Springer-Verlag. URL: https://doi.org/10.1007/978-3-031-72952-2_25.
- Kapadnis, M. N., Patnaik, S., Nandy, A., Ray, S., Goyal, P. and Sheet, D. (2024) Serpent-vlm : Self-refining radiology report generation using vision language models. In *Clinical Natural Language Processing Workshop*. URL: <https://api.semanticscholar.org/CorpusID:269449842>.
- Karmanov, A., Guan, D., Lu, S., El Saddik, A. and Xing, E. (2024a) Efficient test-time adaptation of vision-language models. In *2024 IEEE/CVF Conference on Computer Vision and Pattern Recognition (CVPR)*, 14162–14171.
- Karmanov, A., Guan, D., Lu, S., Saddik, A. E. and Xing, E. (2024b) Efficient test-time adaptation of vision-language models. URL: <https://arxiv.org/abs/2403.18293>.
- Ke, J., He, L., Han, B., Li, J., Wang, D. and Gao, X. (2024) Vldadaptor: Domain adaptive object detection with vision-language model distillation. *IEEE Transactions on Multimedia*, **26**, 11316–11331.
- Kembhavi, A., Salvato, M., Kolve, E., Seo, M., Hajishirzi, H. and Farhadi, A. (2016) A diagram is worth a dozen images. *ArXiv*, **abs/1603.07396**. URL: <https://api.semanticscholar.org/CorpusID:2682274>.
- Kendall, A. and Gal, Y. (2017) What uncertainties do we need in bayesian deep learning for computer vision? In *Advances in Neural Information Processing Systems (NeurIPS)*.
- Kim, J., Misu, T., Chen, Y.-T., Tawari, A. and Canny, J. (2019) Grounding human-to-vehicle advice for self-driving vehicles. In *The IEEE Conference on Computer Vision and Pattern Recognition (CVPR)*.
- Kim, J., Rohrbach, A., Darrell, T., Canny, J. and Akata, Z. (2018) Textual explanations for self-driving vehicles. *Proceedings of the European Conference on Computer Vision (ECCV)*.
- Kim, W., Son, B. and Kim, I. (2021) Vilt: Vision-and-language transformer without convolution or region supervision. In *International Conference on Machine Learning*. URL: <https://api.semanticscholar.org/CorpusID:231839613>.
- Kimura, M. and Bondell, H. D. (2024) Test-time augmentation meets variational bayes. *ArXiv*, **abs/2409.12587**. URL: <https://api.semanticscholar.org/CorpusID:272753370>.
- Klema, V. and Laub, A. (1980) The singular value decomposition: Its computation and some applications. *IEEE Transactions on Automatic Control*, **25**, 164–176.
- Kojima, Y., Xu, J., Zou, X. and Wang, X. (2025) Lora-ttt: Low-rank test-time training for vision-language models. URL: <https://arxiv.org/abs/2502.02069>.
- Kumar, R., Patbhaje, U. and Kumar, A. (2022) An efficient technique for image compression and quality retrieval using matrix completion. *Journal of King Saud University - Computer and Information Sciences*, **34**, 1231–1239. URL: <https://www.sciencedirect.com/science/article/pii/S1319157819302460>.
- Lester, B., Al-Rfou, R. and Constant, N. (2021) The power of scale for parameter-efficient prompt tuning. In *Proceedings of the 2021 Conference on Empirical Methods in Natural Language Processing* (eds. M.-F. Moens, X. Huang, L. Specia and S. W.-t. Yih), 3045–3059. Online and Punta Cana, Dominican Republic: Association for Computational Linguistics. URL: <https://aclanthology.org/2021.emnlp-main.243/>.
- Lewis, A., White, M., Liu, J., Koike-Akino, T., Parsons, K. and Wang, Y. (2025) Winning big with small models: Knowledge distillation vs. self-training for reducing hallucination in qa agents. URL: <https://arxiv.org/abs/2502.19545>.
- Li, B., Wang, R., Wang, G., Ge, Y., Ge, Y. and Shan, Y. (2023) Seed-bench: Benchmarking multimodal llms with generative comprehension. URL: <https://arxiv.org/abs/2307.16125>.
- Li, D., Qin, H., Wu, M., Tang, J., Cao, Y., Wei, C. and Liu, Q. (2024a) Realmind: Advancing visual decoding and language interaction via eeg signals. URL: <https://arxiv.org/abs/2410.23754>.
- Li, J., Li, D., Xiong, C. and Hoi, S. C. H. (2022a) Blip: Bootstrapping language-image pre-training for unified vision-language understanding and generation. In *International Conference on Machine Learning*. URL: <https://api.semanticscholar.org/CorpusID:246411402>.
- Li, L. H., Yatskar, M., Yin, D., Hsieh, C.-J. and Chang, K.-W. (2019) Visualbert: A simple and performant baseline for vision and language. URL: <https://arxiv.org/abs/1908.03557>.
- Li, S., Hu, Y., Ning, X., Liu, X., Hong, K., Jia, X., Li, X., Yan, Y., Ran, P., Dai, G., Yan, S., Yang, H. and Wang, Y. (2024b) Mbq: Modality-balanced quantization for large vision-language models. URL: <https://arxiv.org/abs/2412.19509>.

- Li, X., Yin, X., Li, C., Zhang, P., Hu, X., Zhang, L., Wang, L., Hu, H., Dong, L., Wei, F., Choi, Y. and Gao, J. (2020) Oscar: Object-semantics aligned pre-training for vision-language tasks. In *Computer Vision – ECCV 2020: 16th European Conference, Glasgow, UK, August 23–28, 2020, Proceedings, Part XXX*, 121–137. Berlin, Heidelberg: Springer-Verlag. URL: https://doi.org/10.1007/978-3-030-58577-8_8.
- Li, X. L. and Liang, P. (2021) Prefix-tuning: Optimizing continuous prompts for generation. In *Proceedings of the 59th Annual Meeting of the Association for Computational Linguistics and the 11th International Joint Conference on Natural Language Processing (Volume 1: Long Papers)* (eds. C. Zong, F. Xia, W. Li and R. Navigli), 4582–4597. Online: Association for Computational Linguistics. URL: <https://aclanthology.org/2021.acl-long.353/>.
- Li, Y., Xiong, B., Chen, G. and Chen, Y. (2024c) Setar: Out-of-distribution detection with selective low-rank approximation. URL: <https://arxiv.org/abs/2406.12629>.
- Li, Z., Hou, Z., Liu, H., Li, T., Yang, C., Wang, Y., Shi, C., Xie, L., Zhang, W., Xu, L. and Liu, Z. (2024d) Federated learning in large model era: Vision-language model for smart city safety operation management. In *Companion Proceedings of the ACM Web Conference 2024, WWW '24*, 1578–1585. New York, NY, USA: Association for Computing Machinery. URL: <https://doi.org/10.1145/3589335.3651939>.
- Li, Z., Li, X., Fu, X., Zhang, X., Wang, W., Chen, S. and Yang, J. (2024e) Promptkd: Unsupervised prompt distillation for vision-language models. In *Proceedings of the IEEE/CVF Conference on Computer Vision and Pattern Recognition (CVPR)*, 26617–26626.
- Li, Z., Wang, P., Wang, Z. and Cheng, J. (2021) Fixed-point quantization for vision transformer. In *2021 China Automation Congress (CAC)*, 7282–7287.
- Li, Z., Yang, T., Wang, P. and Cheng, J. (2022b) Q-vit: Fully differentiable quantization for vision transformer. *ArXiv, abs/2201.07703*. URL: <https://api.semanticscholar.org/CorpusID:246035548>.
- Liao, B., Tan, S. and Monz, C. (2023) Make pre-trained model reversible: from parameter to memory efficient fine-tuning. In *Proceedings of the 37th International Conference on Neural Information Processing Systems, NIPS '23*. Red Hook, NY, USA: Curran Associates Inc.
- Lin, H., Bai, H., Liu, Z., Hou, L., Sun, M., Song, L., Wei, Y. and Surr, Z. (2024a) MoPE-CLIP: Structured Pruning for Efficient Vision-Language Models with Module-Wise Pruning Error Metric. In *2024 IEEE/CVF Conference on Computer Vision and Pattern Recognition (CVPR)*, 27360–27370. Los Alamitos, CA, USA: IEEE Computer Society. URL: <https://doi.ieeecomputersociety.org/10.1109/CVPR52733.2024.02584>.
- Lin, T.-Y., Maire, M., Belongie, S., Bourdev, L., Girshick, R., Hays, J., Perona, P., Ramanan, D., Zitnick, C. L. and Dollár, P. (2015) Microsoft coco: Common objects in context. URL: <https://arxiv.org/abs/1405.0312>.
- Lin, W., Zhao, Z., Zhang, X., Wu, C., Zhang, Y., Wang, Y. and Xie, W. (2023) Pmc-clip: Contrastive language-image pre-training using biomedical documents. In *Medical Image Computing and Computer Assisted Intervention – MICCAI 2023: 26th International Conference, Vancouver, BC, Canada, October 8–12, 2023, Proceedings, Part VIII*, 525–536. Berlin, Heidelberg: Springer-Verlag. URL: https://doi.org/10.1007/978-3-031-43993-3_51.
- Lin, Y., Zhang, T., Sun, P., Li, Z. and Zhou, S. (2022) Fq-vit: Post-training quantization for fully quantized vision transformer. In *Proceedings of the Thirty-First International Joint Conference on Artificial Intelligence, IJCAI 2022, Vienna, Austria, 23–29 July 2022* (ed. L. D. Raedt), 1173–1179. ijcai.org. URL: <https://doi.org/10.24963/ijcai.2022/164>.
- Lin, Z., Hu, X., Zhang, Y., Chen, Z., Fang, Z., Chen, X., Li, A., Vepakomma, P. and Gao, Y. (2024b) Splitlora: A split parameter-efficient fine-tuning framework for large language models. URL: <https://arxiv.org/abs/2407.00952>.
- Liu, H. (2024) Simplifying clip: Unleashing the power of large-scale models on consumer-level computers.
- Liu, X., Liu, T., Huang, S., Xin, Y., Hu, Y., Yin, Q., Wang, D. and Chen, H. (2024a) M²ist: Multi-modal interactive side-tuning for efficient referring expression comprehension. URL: <https://arxiv.org/abs/2407.01131>.
- Liu, Y., Duan, H., Zhang, Y., Li, B., Zhang, S., Zhao, W., Yuan, Y., Wang, J., He, C., Liu, Z., Chen, K. and Lin, D. (2023a) Mmbench: Is your multi-modal model an all-around player? *arXiv:2307.06281*.
- Liu, Y., Li, Z., Huang, M., Yang, B., Yu, W., Li, C., Yin, X.-C., Liu, C.-L., Jin, L. and Bai, X. (2024b) Ocrbench: on the hidden mystery of ocr in large multimodal models. *Science China Information Sciences*, **67**. URL: <http://dx.doi.org/10.1007/s11432-024-4235-6>.
- Liu, Y., Wu, C., Tseng, S.-Y., Lal, V., He, X. and Duan, N. (2022) KD-VLP: Improving end-to-end vision-and-language pretraining with object knowledge distillation. In *Findings of the Association for Computational Linguistics: NAACL 2022* (eds. M. Carpuat, M.-C. de Marneffe and I. V. Meza Ruiz), 1589–1600. Seattle, United States: Association for Computational Linguistics. URL: <https://aclanthology.org/2022.findings-naacl.119/>.
- Liu, Y., Yang, H., Dong, Z., Keutzer, K., Du, L. and Zhang, S. (2023b) Noisyquant: Noisy bias-enhanced post-training activation quantization for vision transformers. In *2023 IEEE/CVF Conference on Computer Vision and Pattern Recognition (CVPR)*, 20321–20330.
- Liu, Z., Oğuz, B., Zhao, C., Chang, E., Stock, P., Mehdad, Y., Shi, Y., Krishnamoorthi, R. and Chandra, V. (2023c) Llm-qat: Data-free quantization aware training for large language models. *ArXiv, abs/2305.17888*. URL:

- <https://api.semanticscholar.org/CorpusID:258959117>.
- Liu, Z., Wang, Y., Han, K., Ma, S. and Gao, W. (2021) Post-training quantization for vision transformer. URL: <https://arxiv.org/abs/2106.14156>.
- Lu, H., Zhao, C., Xue, J., Yao, L., Moore, K. and Gong, D. (2025) Adaptive rank, reduced forgetting: Knowledge retention in continual learning vision-language models with dynamic rank-selective lora. URL: <https://arxiv.org/abs/2412.01004>.
- Lu, J., Xiong, C., Parikh, D. and Socher, R. (2016) Knowing when to look: Adaptive attention via a visual sentinel for image captioning. 2017 *IEEE Conference on Computer Vision and Pattern Recognition (CVPR)*, 3242–3250. URL: <https://api.semanticscholar.org/CorpusID:18347865>.
- Lu, P., Bansal, H., Xia, T., Liu, J., Li, C., Hajishirzi, H., Cheng, H., Chang, K.-W., Galley, M. and Gao, J. (2024) Mathvista: Evaluating mathematical reasoning of foundation models in visual contexts. URL: <https://arxiv.org/abs/2310.02255>.
- Lu, P., Mishra, S., Xia, T., Qiu, L., Chang, K.-W., Zhu, S.-C., Tafjord, O., Clark, P. and Kalyan, A. (2022) Learn to explain: multimodal reasoning via thought chains for science question answering. In *Proceedings of the 36th International Conference on Neural Information Processing Systems, NIPS '22*. Red Hook, NY, USA: Curran Associates Inc.
- Lv, C., Chen, H., Guo, J., Guo, J., Guo, J., Ding, Y., Liu, X., Liu, X. and Liu, X. (2024) Ptq4sam: Post-training quantization for segment anything. In *2024 IEEE/CVF Conference on Computer Vision and Pattern Recognition (CVPR)*, 15941–15951.
- Ma, H., Fan, B., Ng, B. K. and Lam, C.-T. (2024) VI-meta: Vision-language models for multimodal meta-learning. *Mathematics*, 12. URL: <https://www.mdpi.com/2227-7390/12/2/286>.
- MA, X., ZHANG, J., Guo, S. and Xu, W. (2023) Swapprompt: Test-time prompt adaptation for vision-language models. In *Advances in Neural Information Processing Systems* (eds. A. Oh, T. Naumann, A. Globerson, K. Saenko, M. Hardt and S. Levine), vol. 36, 65252–65264. Curran Associates, Inc. URL: https://proceedings.neurips.cc/paper_files/paper/2023/file/cdd0640218a27e9e2c0e52e324e25db0-Paper-Conference.pdf.
- Maaz, M., Rasheed, H., Khan, S. and Khan, F. (2024) Video-ChatGPT: Towards detailed video understanding via large vision and language models. In *Proceedings of the 62nd Annual Meeting of the Association for Computational Linguistics (Volume 1: Long Papers)* (eds. L.-W. Ku, A. Martins and V. Srikumar), 12585–12602. Bangkok, Thailand: Association for Computational Linguistics. URL: <https://aclanthology.org/2024.acl-long.679/>.
- Malla, S., Choi, C., Dwivedi, I., Choi, J. H. and Li, J. (2023) Drama: Joint risk localization and captioning in driving. In *Proceedings of the IEEE/CVF Winter Conference on Applications of Computer Vision*, 1043–1052.
- Malladi, S., Gao, T., Nichani, E., Damian, A., Lee, J. D., Chen, D. and Arora, S. (2024) Fine-tuning language models with just forward passes. URL: <https://arxiv.org/abs/2305.17333>.
- Manli, S., Weili, N., De-An, H., Zhiding, Y., Tom, G., Anima, A. and Chaowei, X. (2022) Test-time prompt tuning for zero-shot generalization in vision-language models. In *NeurIPS*.
- Marafioti, A., Farré, M. and Noyan, M. (2025) Smolvlm grows smaller – introducing the 250m & 500m models! <https://huggingface.co/blog/smolervlm> Accessed: 2025-02-20.
- Marafioti, A., Noyan, M., Farre, M., Bakouch, E. and Cuenca, P. (a) Smolvlm - small yet mighty vision language model. <https://huggingface.co/blog/smolvlm#benchmarks>.
- (b) Smolvlm - small yet mighty vision language model. https://huggingface.co/OpenGVLab/InternVL2_5-2B.
- Masry, A., Long, D. X., Tan, J. Q., Joty, S. and Hoque, E. (2022) ChartQA: A benchmark for question answering about charts with visual and logical reasoning. In *Findings of the Association for Computational Linguistics: ACL 2022* (eds. S. Muresan, P. Nakov and A. Villavicencio), 2263–2279. Dublin, Ireland: Association for Computational Linguistics. URL: <https://aclanthology.org/2022.findings-acl.177/>.
- Mathew, M., Karatzas, D. and Jawahar, C. V. (2021) Docvqa: A dataset for vqa on document images. In *2021 IEEE Winter Conference on Applications of Computer Vision (WACV)*, 2199–2208.
- McGrath, M. J., Duenser, A., Lacey, J. and Paris, C. (2024) Collaborative human-ai trust (chai-t): A process framework for active management of trust in human-ai collaboration. URL: <https://arxiv.org/abs/2404.01615>.
- McMahan, H. B., Moore, E., Ramage, D., Hampson, S. and y Arcas, B. A. (2016) Communication-efficient learning of deep networks from decentralized data. In *International Conference on Artificial Intelligence and Statistics*. URL: <https://api.semanticscholar.org/CorpusID:14955348>.
- Meng, X., Ibrahim, S., Behdin, K., Hazimeh, H., Ponomareva, N. and Mazumder, R. (2024) Oscar: one-shot structured pruning in vision and language models with combinatorial optimization. In *Proceedings of the 41st International Conference on Machine Learning, ICML'24*. JMLR.org.
- Mercea, O.-B., Gritsenko, A. A., Schmid, C. and Arnab, A. (2024) Time-, memory- and parameter-efficient visual adaptation. 2024 *IEEE/CVF Conference on Computer Vision and Pattern Recognition (CVPR)*, 5536–5545. URL: <https://api.semanticscholar.org/CorpusID:267412123>.
- Moon, J. H., Lee, H., Shin, W., Kim, Y.-H. and Choi, E. (2022) Multi-modal understanding and generation for medical images and text via vision-language pre-training. *IEEE Journal of Biomedical and Health Informatics*, 26, 6070–6080.
- Nair, P., Datta, P., Dean, J., Jain, P. and Kusupati, A. (2025) Matryoshka quantization. URL: <https://arxiv.org/abs/2502.06786>.

- Najdenkoska, I., Zhen, X. and Worring, M. (2023) Meta learning to bridge vision and language models for multimodal few-shot learning. URL: <https://arxiv.org/abs/2302.14794>.
- Nie, F., Hu, Z. and Li, X. (2019) Matrix completion based on non-convex low-rank approximation. *IEEE Transactions on Image Processing*, **28**, 2378–2388.
- Nie, Y., He, W., Han, K., Tang, Y., Guo, T., Du, F. and Wang, Y. (2023) Lightclip: Learning multi-level interaction for lightweight vision-language models. URL: <https://arxiv.org/abs/2312.00674>.
- Okamura, K. and Yamada, S. (2020) Adaptive trust calibration for human-ai collaboration. *PLOS ONE*, **15**, 1–20. URL: <https://doi.org/10.1371/journal.pone.0229132>.
- Pan, B., Huang, W. and Shi, Y. (2024) Federated learning from vision-language foundation models: Theoretical analysis and method. In *Advances in Neural Information Processing Systems* (eds. A. Globerson, L. Mackey, D. Belgrave, A. Fan, U. Paquet, J. Tomczak and C. Zhang), vol. 37, 30590–30623. Curran Associates, Inc. URL: https://proceedings.neurips.cc/paper_files/paper/2024/file/36721d1209a059dcb7a090dd543f34c4-Paper-Conference.pdf.
- Park, S., Lee, M., Kang, J., Choi, H., Park, Y., Cho, J., Lee, A. and Kim, D. (2024) Vlaad: Vision and language assistant for autonomous driving. In *2024 IEEE/CVF Winter Conference on Applications of Computer Vision Workshops (WACVW)*, 980–987.
- Qwen, ; Yang, A., Yang, B., Zhang, B., Hui, B., Zheng, B., Yu, B., Li, C., Liu, D., Huang, F., Wei, H., Lin, H., Yang, J., Tu, J., Zhang, J., Yang, J., Yang, J., Zhou, J., Lin, J., Dang, K., Lu, K., Bao, K., Yang, K., Yu, L., Li, M., Xue, M., Zhang, P., Zhu, Q., Men, R., Lin, R., Li, T., Xia, T., Ren, X., Ren, X., Fan, Y., Su, Y., Zhang, Y., Wan, Y., Liu, Y., Cui, Z., Zhang, Z. and Qiu, Z. (2024) Qwen2.5 technical report. URL: <https://arxiv.org/abs/2412.15115>.
- Radford, A., Kim, J. W., Hallacy, C., Ramesh, A., Goh, G., Agarwal, S., Sastry, G., Askell, A., Mishkin, P., Clark, J., Krueger, G. and Sutskever, I. (2021) Learning transferable visual models from natural language supervision. In *International Conference on Machine Learning*. URL: <https://api.semanticscholar.org/CorpusID:231591445>.
- Radford, A., Wu, J., Child, R., Luan, D., Amodei, D. and Sutskever, I. (2019) Language models are unsupervised multitask learners. URL: <https://api.semanticscholar.org/CorpusID:160025533>.
- Ren, T., Liu, S., Zeng, A., Lin, J., Li, K., Cao, H., Chen, J., Huang, X., Chen, Y., Yan, F., Zeng, Z., Zhang, H., Li, F., Yang, J., Li, H., Jiang, Q. and Zhang, L. (2024) Grounded sam: Assembling open-world models for diverse visual tasks. URL: <https://arxiv.org/abs/2401.14159>.
- Sameni, S., Kafle, K., Tan, H. and Jenni, S. (2024) Building vision-language models on solid foundations with masked distillation. In *Proceedings of the IEEE/CVF Conference on Computer Vision and Pattern Recognition (CVPR)*, 14216–14226.
- Selvaraju, R. R., Cogswell, M., Das, A., Vedantam, R., Parikh, D. and Batra, D. (2017) Grad-cam: Visual explanations from deep networks via gradient-based localization. In *Proceedings of the IEEE International Conference on Computer Vision (ICCV)*.
- Sharma, P., Ding, N., Goodman, S. and Soricut, R. (2018) Conceptual captions: A cleaned, hypernymed, image alt-text dataset for automatic image captioning. In *Proceedings of the 56th Annual Meeting of the Association for Computational Linguistics (Volume 1: Long Papers)* (eds. I. Gurevych and Y. Miyao), 2556–2565. Melbourne, Australia: Association for Computational Linguistics. URL: <https://aclanthology.org/P18-1238/>.
- Sharshar, A., Khan, L. U., Ullah, W. and Guizani, M. (2025) Vision-language models for edge networks: A comprehensive survey. URL: <https://arxiv.org/abs/2502.07855>.
- Shen, S., Yao, Z., Li, C., Darrell, T., Keutzer, K. and He, Y. (2023) Scaling vision-language models with sparse mixture of experts. In *Findings of the Association for Computational Linguistics: EMNLP 2023* (eds. H. Bouamor, J. Pino and K. Bali), 11329–11344. Singapore: Association for Computational Linguistics. URL: <https://aclanthology.org/2023.findings-emnlp.758/>.
- Silva, U. D., Fernando, L., Lik, B. L. P., Koh, Z., Joyce, S. C., Yuen, B. and Yuen, C. (2025) Large language models for video surveillance applications. URL: <https://arxiv.org/abs/2501.02850>.
- Singh, A., Hu, R., Goswami, V., Couairon, G., Galuba, W., Rohrbach, M. and Kiela, D. (2022) Flava: A foundational language and vision alignment model. In *2022 IEEE/CVF Conference on Computer Vision and Pattern Recognition (CVPR)*, 15617–15629.
- Singh, A., Natarajan, V., Shah, M., Jiang, Y., Chen, X., Batra, D., Parikh, D. and Rohrbach, M. (2019) Towards vqa models that can read. In *2019 IEEE/CVF Conference on Computer Vision and Pattern Recognition (CVPR)*, 8309–8318.
- Song, D., Liang, J., Payandeh, A., Raj, A. H., Xiao, X. and Manocha, D. (2025) Vlm-social-nav: Socially aware robot navigation through scoring using vision-language models. *IEEE Robotics and Automation Letters*, **10**, 508–515.
- Song, L., Chen, Y., Yang, S., Ding, X., Ge, Y., Chen, Y.-C. and Shan, Y. (2024a) Low-rank approximation for sparse attention in multi-modal llms. In *2024 IEEE/CVF Conference on Computer Vision and Pattern Recognition (CVPR)*, 13763–13773.
- Song, Y., Paperno, D. and Gatt, A. (2024b) Context-aware visual storytelling with visual prefix tuning and contrastive learning. In *Proceedings of the 17th International Natural Language Generation Conference* (eds. S. Mahamood, N. L. Minh and D. Ippolito), 384–401. Tokyo, Japan: Association for Computational Linguistics. URL: <https://aclanthology.org/2024.inlg-main.32/>.
- van Sonsbeek, T., Derakhshani, M. M., Najdenkoska, I., Snoek, C. G. M. and Worring, M. (2023) Open-ended medical visual question answering through prefix tuning of language models. In *Medical Image Computing and Computer Assisted Intervention - MICCAI 2023: 26th International Conference, Vancouver, BC, Canada, October 8–12, 2023, Proceedings, Part V*, 726–736. Berlin, Heidelberg: Springer-Verlag. URL: https://doi.org/10.1007/978-3-031-43904-9_70.

- Stover, D. and Bowman, D. (2024) Taggar: General-purpose task guidance from natural language in augmented reality using vision-language models. In *Proceedings of the 2024 ACM Symposium on Spatial User Interaction*, SUI '24. New York, NY, USA: Association for Computing Machinery. URL: <https://doi.org/10.1145/3677386.3682095>.
- Subramanian, S., Wang, L. L., Mehta, S., Bogin, B., van Zuylen, M., Parasa, S., Singh, S., Gardner, M. and Hajishirzi, H. (2020) MediCaT: A Dataset of Medical Images, Captions, and Textual References. In *Findings of EMNLP*.
- Sun, H., Wang, R., Li, Y., Cao, X., Jiang, X., Hu, Y. and Zhang, B. (2024) P4q: Learning to prompt for quantization in visual-language models. URL: <https://arxiv.org/abs/2409.17634>.
- Sun, Y. and Ochiai, H. (2024) Bidirectional contrastive split learning for visual question answering. In *Proceedings of the Thirty-Eighth AAAI Conference on Artificial Intelligence and Thirty-Sixth Conference on Innovative Applications of Artificial Intelligence and Fourteenth Symposium on Educational Advances in Artificial Intelligence*, AAAI'24/IAAI'24/EAAI'24. AAAI Press. URL: <https://doi.org/10.1609/aaai.v38i19.30158>.
- Sung, Y.-L., Cho, J. and Bansal, M. (2022) Vi-adapter: Parameter-efficient transfer learning for vision-and-language tasks. In *2022 IEEE/CVF Conference on Computer Vision and Pattern Recognition (CVPR)*, 5217–5227.
- Tallam, K. (2025) From autonomous agents to integrated systems, a new paradigm: Orchestrated distributed intelligence. URL: <https://arxiv.org/abs/2503.13754>.
- Tang, N., Fu, M. and Wu, J. (2024) Minimal interaction edge tuning: A new paradigm for visual adaptation. URL: <https://arxiv.org/abs/2406.17559>.
- Team, C. (2024) Chameleon: Mixed-modal early-fusion foundation models. *ArXiv*, abs/2405.09818. URL: <https://api.semanticscholar.org/CorpusID:269791516>.
- Tian, X., Gu, J., Li, B., Liu, Y., Hu, C., Wang, Y., Zhan, K., Jia, P., Lang, X. and Zhao, H. (2024) DriveVlm: The convergence of autonomous driving and large vision-language models. *ArXiv*, abs/2402.12289. URL: <https://api.semanticscholar.org/CorpusID:267750682>.
- Tran, L., Sun, W., Patterson, S. and Milanova, A. (2025) Privacy-preserving personalized federated prompt learning for multi-modal large language models. URL: <https://arxiv.org/abs/2501.13904>.
- Tsimpoukelli, M., Menick, J., Cabi, S., Eslami, S. M. A., Vinyals, O., Hill, F. and Janssen, Z. (2021) Multimodal few-shot learning with frozen language models. *ArXiv*, abs/2106.13884. URL: <https://api.semanticscholar.org/CorpusID:235658331>.
- Vasu, P. K. A., Faghri, F., Li, C.-L., Koc, C., True, N., Antony, A., Santhanam, G., Gabriel, J., Grasc, P., Tuzel, O. and Pouransari, H. (2025) FastVlm: Efficient vision encoding for vision language models. In *Proceedings of the IEEE/CVF Conference on Computer Vision and Pattern Recognition (CVPR)*.
- Vaswani, A., Shazeer, N. M., Parmar, N., Uszkoreit, J., Jones, L., Gomez, A. N., Kaiser, L. and Polosukhin, I. (2017) Attention is all you need. In *Neural Information Processing Systems*. URL: <https://api.semanticscholar.org/CorpusID:13756489>.
- Wang, C., Wang, Z., Xu, X., Tang, Y., Zhou, J. and Lu, J. (2024) Q-vlm: Post-training quantization for large vision-language models. URL: <https://arxiv.org/abs/2410.08119>.
- Wang, J., Hu, X., Zhang, P., Li, X., Wang, L., Zhang, L., Gao, J. and Liu, Z. (2021) MiniVlm: A smaller and faster vision-language model. URL: <https://arxiv.org/abs/2012.06946>.
- Wang, T., Zhou, W., Zeng, Y. and Zhang, X. (2023a) EfficientVlm: Fast and accurate vision-language models via knowledge distillation and modal-adaptive pruning. In *Findings of the Association for Computational Linguistics: ACL 2023, Toronto, Canada, July 9-14, 2023* (eds. A. Rogers, J. L. Boyd-Graber and N. Okazaki), 13899–13913. Association for Computational Linguistics. URL: <https://doi.org/10.18653/v1/2023.findings-acl.873>.
- Wang, W., Gao, Z., Chen, L., Chen, Z., Zhu, J., Zhao, X., Liu, Y., Cao, Y., Ye, S., Zhu, X., Lu, L., Duan, H., Qiao, Y., Dai, J. and Wang, W. (2025a) Visualprm: An effective process reward model for multimodal reasoning. URL: <https://arxiv.org/abs/2503.10291>.
- Wang, W., Lai, Z., Li, S., Liu, W., Ge, K., Liu, Y., Shen, A. and Li, D. (2023b) Prophet: Fine-grained load balancing for parallel training of large-scale moe models. In *2023 IEEE International Conference on Cluster Computing (CLUSTER)*, 82–94.
- Wang, X., Wang, G., Chai, W., Zhou, J. and Wang, G. (2023c) User-aware prefix-tuning is a good learner for personalized image captioning. In *Pattern Recognition and Computer Vision: 6th Chinese Conference, PRCV 2023, Xiamen, China, October 13–15, 2023, Proceedings, Part VII*, 384–395. Berlin, Heidelberg: Springer-Verlag. URL: https://doi.org/10.1007/978-981-99-8540-1_31.
- Wang, Z., Chen, J., Zhou, W., Zhu, H., Liang, J., Shan, L., Liu, M., Xu, D., Yang, Q. and Qin, B. (2023d) Smarttrim: Adaptive tokens and attention pruning for efficient vision-language models. In *International Conference on Language Resources and Evaluation*. URL: <https://api.semanticscholar.org/CorpusID:268032404>.
- Wang, Z., Dai, J., Li, K., Li, X., Guo, Y. and Xiang, M. (2025b) Complementary subspace low-rank adaptation of vision-language models for few-shot classification. URL: <https://arxiv.org/abs/2501.15040>.
- Wiyatno, R. R. and Xu, A. (2018) Maximal jacobian-based saliency map attack. *ArXiv*, abs/1808.07945. URL: <https://api.semanticscholar.org/CorpusID:52091347>.
- Xiao, G., Lin, J., Seznec, M., Wu, H., Demouth, J. and Han, S. (2023) Smoothquant: accurate and efficient post-training quantiza-

- tion for large language models. In *Proceedings of the 40th International Conference on Machine Learning, ICML'23*. JMLR.org.
- Xie, J., Zhang, Y., Lin, M., Cao, L. and Ji, R. (2024a) Advancing multimodal large language models with quantization-aware scale learning for efficient adaptation. In *Proceedings of the 32nd ACM International Conference on Multimedia, MM '24*, 10582–10591. New York, NY, USA: Association for Computing Machinery. URL: <https://doi.org/10.1145/3664647.3680838>.
- Xie, Z., Yu, S., He, Q. and Li, M. (2024b) Sonic visionlm: Playing sound with vision language models. In *2024 IEEE/CVF Conference on Computer Vision and Pattern Recognition (CVPR)*, 26856–26865.
- Xing, J., Liu, J., Wang, J., Sun, L., Chen, X., Gu, X. and Wang, Y. (2024a) A survey of efficient fine-tuning methods for vision-language models – prompt and adapter. *Comput. Graph.*, **119**. URL: <https://doi.org/10.1016/j.cag.2024.01.012>.
- Xing, Y., Wu, Q., Cheng, D., Zhang, S., Liang, G., Wang, P. and Zhang, Y. (2024b) Dual modality prompt tuning for vision-language pre-trained model. *Trans. Multi.*, **26**, 2056–2068. URL: <https://doi.org/10.1109/TMM.2023.3291588>.
- Xiu, Y., Scargill, T. and Gorlatova, M. (2025) Viddar: Vision language model-based task-detrimental content detection for augmented reality. URL: <https://arxiv.org/abs/2501.12553>.
- Xu, J., Mei, T., Yao, T. and Rui, Y. (2016) Msr-vtt: A large video description dataset for bridging video and language. In *2016 IEEE Conference on Computer Vision and Pattern Recognition (CVPR)*, 5288–5296.
- Xu, W., Liu, Y., He, L., Huang, X. and Jiang, L. (2024) Xmodel-vlm: A simple baseline for multimodal vision language model. URL: <https://arxiv.org/abs/2405.09215>.
- Xu, Y., Xie, L., Gu, X., Chen, X., Chang, H., Zhang, H., Chen, Z., Zhang, X. and Tian, Q. (2023) Qa-lora: Quantization-aware low-rank adaptation of large language models. URL: <https://arxiv.org/abs/2309.14717>.
- Yan, H. and Guo, Y. (2024) Lightweight unsupervised federated learning with pretrained vision language model. URL: <https://arxiv.org/abs/2404.11046>.
- Yang, L., Zhang, R.-Y., Wang, Y. and Xie, X. (2024) Mma: Multi-modal adapter for vision-language models. In *2024 IEEE/CVF Conference on Computer Vision and Pattern Recognition (CVPR)*, 23826–23837.
- Yang, P. and Dong, B. (2025) Mocoll: Agent-based specific and general model collaboration for image captioning. URL: <https://arxiv.org/abs/2501.01834>.
- Yang, S., Tang, H., Lin, J., Tang, J., Chen, W.-M., Wang, W.-C., Xiao, G., Dang, X., Gan, C. and Han, S. () Tinychat: Visual language models & edge ai 2.0. <https://hanlab.mit.edu/blog/tinychat-vlm>
- Yang, T., Li, Z., Cao, J. and Xu, C. (2025) Mitigating hallucination in large vision-language models via modular attribution and intervention. In *The Thirteenth International Conference on Learning Representations*. URL: <https://openreview.net/forum?id=Bjq4W7P2Us>.
- Yao, H., Zhang, R. and Xu, C. (2023) Visual-language prompt tuning with knowledge-guided context optimization. In *2023 IEEE/CVF Conference on Computer Vision and Pattern Recognition (CVPR)*, 6757–6767.
- Yi-Lin Sung, Jaehong Yoon, M. B. (2024) Ecoflap: Efficient coarse-to-fine layer-wise pruning for vision-language models. In *International Conference on Learning Representations (ICLR)*.
- Yoon, H. S., Yoon, E., Tee, J. T. J., Hasegawa-Johnson, M. A., Li, Y. and Yoo, C. D. (2024) C-TPT: Calibrated test-time prompt tuning for vision-language models via text feature dispersion. In *The Twelfth International Conference on Learning Representations*. URL: <https://openreview.net/forum?id=jzzEHTBF0T>.
- You, J., Shi, H., Jiang, Z., Huang, Z., Gan, R., Wu, K., Cheng, X., Li, X. and Ran, B. (2024) V2x-vlm: End-to-end v2x cooperative autonomous driving through large vision-language models. *ArXiv*, **abs/2408.09251**. URL: <https://api.semanticscholar.org/CorpusID:271903020>.
- Yu, C., Chen, T., Gan, Z. and Fan, J. (2023a) Boost vision transformer with gpu-friendly sparsity and quantization. In *2023 IEEE/CVF Conference on Computer Vision and Pattern Recognition (CVPR)*, 22658–22668.
- Yu, J., Zhuge, Y., Zhang, L., Hu, P., Wang, D., Lu, H. and He, Y. (2024) Boosting continual learning of vision-language models via mixture-of-experts adapters. In *Proceedings of the IEEE/CVF Conference on Computer Vision and Pattern Recognition*, 23219–23230.
- Yu, L., Shi, B., Pasunuru, R., Muller, B., Golovneva, O., Wang, T., Babu, A., Tang, B., Karrer, B., Sheynin, S., Ross, C., Polyak, A., Howes, R., Sharma, V., Xu, P., Tamoyan, H., Ashual, O., Singer, U., Li, S.-W. and Aghajanyan, A. (2023b) Scaling autoregressive multi-modal models: Pretraining and instruction tuning.
- Yuan, Z., Xue, C., Chen, Y., Wu, Q. and Sun, G. (2022) Ptq4vit: Post-training quantization for vision transformers with twin uniform quantization. In *Computer Vision – ECCV 2022: 17th European Conference, Tel Aviv, Israel, October 23–27, 2022, Proceedings, Part XII*, 191–207. Berlin, Heidelberg: Springer-Verlag. URL: https://doi.org/10.1007/978-3-031-19775-8_12.
- Yue, X., Ni, Y., Zhang, K., Zheng, T., Liu, R., Zhang, G., Stevens, S., Jiang, D., Ren, W., Sun, Y., Wei, C., Yu, B., Yuan, R., Sun, R., Yin, M., Zheng, B., Yang, Z., Liu, Y., Huang, W., Sun, H., Su, Y. and Chen, W. (2024a) Mmmu: A massive multi-discipline multimodal understanding and reasoning benchmark for expert agi. In *Proceedings of CVPR*.
- (2024b) Mmmu: A massive multi-discipline multimodal understanding and reasoning benchmark for expert agi. URL:

- <https://arxiv.org/abs/2311.16502>.
- Zanella, M. and Ayed, I. B. (2024a) Low-rank few-shot adaptation of vision-language models. 2024 IEEE/CVF Conference on Computer Vision and Pattern Recognition Workshops (CVPRW), 1593–1603. URL: <https://api.semanticscholar.org/CorpusID:270094592>.
- (2024b) On the test-time zero-shot generalization of vision-language models: Do we really need prompt learning? 2024 IEEE/CVF Conference on Computer Vision and Pattern Recognition (CVPR), 23783–23793. URL: <https://api.semanticscholar.org/CorpusID:269587806>.
- Zeng, H., Yue, Z., Zhang, Y., Shang, L. and Wang, D. (2024) Fair federated learning with biased vision-language models. In *Findings of the Association for Computational Linguistics: ACL 2024* (eds. L.-W. Ku, A. Martins and V. Srikumar), 10002–10017. Bangkok, Thailand: Association for Computational Linguistics. URL: <https://aclanthology.org/2024.findings-acl.595/>.
- Zhai, X., Mustafa, B., Kolesnikov, A. and Beyer, L. (2023) Sigmoid loss for language image pre-training. In *2023 IEEE/CVF International Conference on Computer Vision (ICCV)*, 11941–11952.
- Zhang, J., Huang, H., Zhang, P., Wei, J., Zhu, J. and Chen, J. (2025a) Sageattention2: Efficient attention with thorough outlier smoothing and per-thread int4 quantization. In *International Conference on Machine Learning (ICML)*.
- Zhang, J., Huang, J., Jin, S. and Lu, S. (2024a) Vision-language models for vision tasks: A survey. *IEEE Transactions on Pattern Analysis and Machine Intelligence*, **46**, 5625–5644.
- (2024b) Vision-language models for vision tasks: A survey. *IEEE Transactions on Pattern Analysis and Machine Intelligence*, **46**, 5625–5644.
- Zhang, J., Ma, X., Wang, X., Qiu, L., Wang, J., Jiang, Y.-G. and Sang, J. (2024c) Adversarial prompt tuning for vision-language models. In *Computer Vision – ECCV 2024: 18th European Conference, Milan, Italy, September 29–October 4, 2024, Proceedings, Part XLV*, 56–72. Berlin, Heidelberg: Springer-Verlag. URL: https://doi.org/10.1007/978-3-031-72995-9_4.
- Zhang, J., Wei, J., Zhang, P., Zhu, J. and Chen, J. (2025b) Sageattention: Accurate 8-bit attention for plug-and-play inference acceleration. In *International Conference on Learning Representations (ICLR)*.
- Zhang, P., Goyal, Y., Summers-Stay, D., Batra, D. and Parikh, D. (2016) Yin and Yang: Balancing and answering binary visual questions. In *Conference on Computer Vision and Pattern Recognition (CVPR)*.
- Zhao, J., Zhang, M., Zeng, C., Wang, M., Liu, X. and Nie, L. (2024) LRQuant: Learnable and robust post-training quantization for large language models. In *Proceedings of the 62nd Annual Meeting of the Association for Computational Linguistics (Volume 1: Long Papers)* (eds. L.-W. Ku, A. Martins and V. Srikumar), 2240–2255. Bangkok, Thailand: Association for Computational Linguistics. URL: <https://aclanthology.org/2024.acl-long.122/>.
- Zheng, P., Zhu, Y., Zhang, Z., Hu, Y. and Schmeink, A. (2021) Federated learning in heterogeneous networks with unreliable communication. In *2021 IEEE Globecom Workshops (GC Wkshps)*, 1–6.
- Zhong, H., Shen, S., Cai, K., Wu, Z., Yao, J., Cheng, Y., Li, X., Zhang, X., Song, L. and Hu, Q. (2025) Serial low-rank adaptation of vision transformer. URL: <https://arxiv.org/abs/2503.17750>.
- Zhou, B., Hu, Y., Weng, X., Jia, J., Luo, J., Liu, X., Wu, J. and Huang, L. (2024) Tinyllava: A framework of small-scale large multimodal models. URL: <https://arxiv.org/abs/2402.14289>.
- Zhou, C., Shen, Q., Yu, Z., Bu, J. and Wang, H. (2025) One head eight arms: Block matrix based low rank adaptation for clip-based few-shot learning. URL: <https://arxiv.org/abs/2501.16720>.
- Zhou, X., Liu, M., Yurtsever, E., Žagar, B. L., Zimmer, W., Cao, H. and Knoll, A. C. (2023) Vision language models in autonomous driving: A survey and outlook. *IEEE Transactions on Intelligent Vehicles*. URL: <https://api.semanticscholar.org/CorpusID:269865211>.
- Zhu, D., Chen, J., Shen, X., Li, X. and Elhoseiny, M. (2023) Minigt-4: Enhancing vision-language understanding with advanced large language models. *ArXiv*, **abs/2304.10592**. URL: <https://api.semanticscholar.org/CorpusID:258291930>.
- Zhu, K., Gu, J., You, Z., Qiao, Y. and Dong, C. (2025) An intelligent agentic system for complex image restoration problems. URL: <https://arxiv.org/abs/2410.17809>.
- Zhu, L., Liu, Z. and Han, S. (2019) *Deep leakage from gradients*. Red Hook, NY, USA: Curran Associates Inc.
- Zhu, Y., Zhang, G., Xu, C., Shen, H., Chen, X., Wu, G. and Wang, L. (2024) Efficient test-time prompt tuning for vision-language models. *CoRR*, **abs/2408.05775**. URL: <https://doi.org/10.48550/arXiv.2408.05775>.